# REPORT DOCUMENTATION PAGE

Form Approved OMB No. 0704-0188

Public reporting burden for this collection of information is estimated to average 1 hour per response, including the time for reviewing instructions, searching existing data sources, gathering and maintaining the data needed, and completing and reviewing the collection of information. Send comments regarding this burden estimate or any other aspect of this collection of information, including suggestions for reducing this burden to Washington Headquarters Services, Directorate for Information Operations and Reports, 1215 Jefferson Davis Highway, Suite 1204, Arlington, VA 22202-4302, and to the Office of Management and Budget, Paperwork Reduction Project (0704-0188), Washington, DC 20503.

| 1. AGENCY USE ONLY (Leave blank) | 2. REPORT DATE | 3. REPORT TYPE AND DATES COVERED |
| --- | --- | --- |
| | 1997 | Final Report |

| 4. TITLE AND SUBTITLE | 5. FUNDING NUMBERS |
| --- | --- |
| The Study Of Possibility To Implement The Dynamic Nonlinear-Optical Corrector Based On The Use Of The Optical Negative-Feedback Loop For Correction For Distortions Of Large Scale Optics | F6170896W0309 |

**6. AUTHOR(S)**

Dr. Vladimir Y. Venediktov

| 7. PERFORMING ORGANIZATION NAME(S) AND ADDRESS(ES) | 8. PERFORMING ORGANIZATION REPORT NUMBER |
| --- | --- |
| Research Institute for Laser Physics<br>Vavilov State Optical Institute<br>Birjevaya, 12<br>St. Petersburg 199034<br>Russia | N/A |

| 9. SPONSORING/MONITORING AGENCY NAME(S) AND ADDRESS(ES) | 10. SPONSORING/MONITORING AGENCY REPORT NUMBER |
| --- | --- |
| EOARD<br>PSC 802 BOX 14<br>FPO 09499-0200 | SPC 96-4094 |

**11. SUPPLEMENTARY NOTES**

| 12a. DISTRIBUTION/AVAILABILITY STATEMENT | 12b. DISTRIBUTION CODE |
| --- | --- |
| Approved for public release; distribution is unlimited. | A |

**13. ABSTRACT (Maximum 200 words)**

This report results from a contract tasking Research Institute for Laser Physics as follows: The contractor will perform a comparative analysis of approaches to overcoming the 2 pi problem in nonlinear optical feedback correction schemes and determine an optimal solution.

| 14. SUBJECT TERMS | 15. NUMBER OF PAGES |
| --- | --- |
| Physics, Non-linear Optics | 67 |
| DTIC QUALITY INSPECTED 4 | 16. PRICE CODE N/A |

| 17. SECURITY CLASSIFICATION OF REPORT | 18. SECURITY CLASSIFICATION OF THIS PAGE | 19. SECURITY CLASSIFICATION OF ABSTRACT | 20. LIMITATION OF ABSTRACT |
| --- | --- | --- | --- |
| UNCLASSIFIED | UNCLASSIFIED | UNCLASSIFIED | UL |

NSN 7540-01-280-5500

Standard Form 298 (Rev. 2-89)
Prescribed by ANSI Std. 239-18
298-102

Institute for Laser Physics of SC "Vavilov State Optical Institute"

&

Company Lasers and Optical System, Ltd.

*SPC96-4094*

*Contract F-61708-96 - W0309*

# The Study of Possibility to implement the Dynamic Nonlinear - Optical Corrector based on the Use of the Optical Negative Feedback Loop for Correction for Distortions of Large Scale Optics

### Final Report

**Director of the Institute**       **Prof. Arthur A.Mak**

**Principle Investigator**       **Vladimir Yu.Venediktov**

St.-Petersburg

*1997*

## *Preface*

This Report is delivered on the completion of the studies in the frame of the Contract #F6170896W0309, carried out by the Company LOS Ltd., St.-Petersburg, Russia with the participation of the scientists of the Research Institute for Laser Physics, St.-Petersburg, Russia, and of the Research Center "Vavilov State Optical Institute", St.-Petersburg, Russia. The work was done by (in alphabetical order) N.A.Bezina, V.A.Berenberg, A.A.Leshchev, A.P.Onohov, A.G.Seregin, L.N.Soms, M.V.Vasil'ev, V.Yu.Venediktov (principle investigator), F.L.Vladimirov.

The fast, cheap and reliable technique of the computations-free, analogous correction for distortions, based on the use of the liquid crystal spatial light modulator (LC SLM), placed into the loop of negative optical feedback is a very promising technique for correction for distortions, imposed by the defects and deformations of the large scale optical elements, as well as by the distortions in the extended atmospheric beamlet. The corrector of such a kind is recorded with the use of the auxiliary laser source and can be applied for correction for distortions in the wide spectral band. However, the practical application of the element is until now limited by the so called $2\pi$-problem (see further), preventing correction for the phase distortions in the wide spectral range with the magnitude of more than one wavelength of visible radiation.

In the Interim Report #1 to the same Contract we have shown that it is possible to expand significantly the range of amplitudes of the wavefront distortions, corrected in the wide spectral range. It can be done by the use in NOF-schematics of the special interferometery scheme, providing the monotonous variation of the intensity in the interference pattern of the nondistorted reference and distorted signal waves with the variation of the distorted wave phase retardation in the range of several radiation wavelengths.

During the second stage of the work, reported in the Interim Report #2, we have continued the analysis of the possibility to implement in practice such an approach to the dynamic correction for wavefront distortions. With this purpose we had, first of all, prepared the brief review of the published results on NOF-correction.

We have also analyzed the technology problems of NOF-correction with the expanded range of distortions amplitude. These are, first of all, the problems, caused

by the necessity to realize the optically addressed deep (several wavelength) phase modulation, as well as the problem of the thin dynamic hologram realization.

We have also started the analysis of possible schematics of the optical system of the experiment on the discussed approach realization; we proposed the improved optical scheme and analyzed the correction abilities of the system.

The results of the first two stages of the work are incorporated into the present Final Report (Chapters 1, 2, 3 and 6).

To the final stage of the work it became clear, that the main efforts are to be concentrated on the technology and realization of the key element of the scheme - the LC SLM with the extremely deep depth of phase modulation (retardation). Basing on the results of the preceding stages we have carried out the more thorough studies in two directions:

1. We have designed, realized and tested in model experiment the prototype of the optically addressed LC SLM, based on the use of novel type of photoconductor layer (chalcogenide glass). The results (see Chapter 4) indicate that the problem of realization of the element with the extremely deep phase retardation in OA LC SLM can be successfully solved. However, the response time of such elements is rather slow.

2. Better response time can be realized in the electrically addressed LC SLM. Such an element can be combined together with the TV-registration contour and thus simulate the optically addressed behavior. This item is analyzed in the Chapter 5.

Summarizing all the results, we got the possibility to outline the scheme of possible demonstration experiment, which is to show the feasibility of the method. This experiment, as well as possible activities on the further elaboration of the technologies involved, are discussed in Chapter 7.

# 1. Introduction

## 1.1. Background and state-of-the-art

In mid-80es there was proposed [1] and realized in several experiments [2,3] the scheme of the nonlinear-optical correction for distortions of optical radiation wavefront, using the optically addressed spatial phase modulator, introduced into the negative optical feedback (NOF) loop (see Fig.1.1).
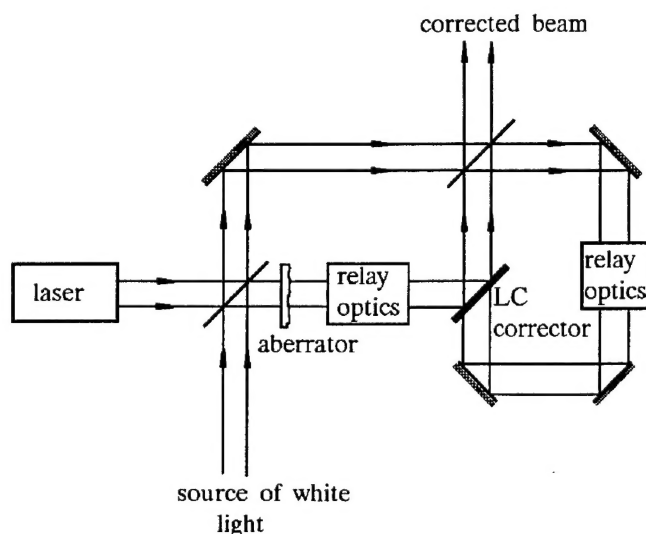


Fig.1.1. Usual scheme of NOF-correction for distortions

In such a scheme the probe beam of radiation of the auxiliary laser source passes via the aberrated optical beamlet and through the layer of controlled optical thickness (the layer of liquid crystal, LC, in the optically addressed spatial light modulator, SLM, [4]). The optical thickness of this layer, i.e. phase delay of the probe beam, depends on the intensity of controlling optical signal coming to the corresponding zone of photoconductor of the SLM. In our case such a signal is the interference pattern of the probe beam with the coherent and coaxial nondistorted reference beam. In this case in the system there is realized the optical feedback. In the case of appropriate phase shift between the probe and reference beams this feedback reveals itself as the negative feedback, and the system as a whole shifts itself into the mode, in which the wavefront distortions, imposed by the induced relief of optical thickness of LC layer, adds approximately to that imposed by the aberrated beamlet and thus corrects for them. Note, that such a corrector works not only at the

wavelength of the auxiliary laser source, but can be (with the accuracy of spectral dispersion of the LC refraction index) used across the overall spectral range of LC transparency.

The basic limitation, preventing this technique use for practical purposes is the so called $2\pi$-problem. In any scheme of the output signal stabilization, using the negative feedback, the maximal magnitude of the error corrected is in the very best case limited by the period of variation of the signal, used for the control of actuator with this error variation. In our case the control signal is produced by the dual beam interference in the Michelson, Mach-Zander etc. interferometer. Correspondingly, the period of variation of the intensity at the output of such an interferometer vs. relative phase shift between the reference and probe wave (i.e., the magnitude of the corrected distortion of wavefront) can not exceed the wavelength of the auxiliary laser source emission.

In the case of larger distortions, exceeding these limitations, the aperture of the corrector splits into several independent domains with the abrupt phase shift at the edge. Such a system is not stable, the acute edges of the domains result in significant diffraction losses of radiation. But the most important disadvantage is that the regions of the corrected wavefront, corresponding to different domains, obtain the relative phase shift in one or several wavelengths. Such a "broken" corrector can be used not in the whole range of LC transparency, but only in the rather narrow spectral zone $\Delta\lambda<<\lambda$ .

There are several possibilities of the system performance improvement so as to enlarge the range of magnitudes of the corrected distortions with the preservation of wide spectral range of corrected radiation wavelengths. For example, some improvement can be obtained just by enlargement of the auxiliary laser source radiation wavelength. However, the significant shift to the mid-IR range of spectrum (several microns) is limited by the reduce of LC media transparency and by the lack of sensitive photoelectric elements.

D.M.Pepper has suggested to use the spectrum-zonal approach. One can split the spectral range of correction into several narrow ranges and to use separate corrector for each of these ranges. This approach, however, is very complicated and

results in significant energy losses due to the necessity of complicated spectral separation.

Recently we have proposed another approach to this problem solution, which seems now to be the most prospective. The simple dual beam interferometer, forming the NOF signal in the discussed schematics, can be replaced by the sophisticated interferometric scheme, in which the variation of the output intensity from minimum to maximum will be smooth and monotonous along the phase shift range, whose magnitude equals several wavelengths of probe radiation.

Such an interferometer can, in particular, implement the following property of the thin (plain, non-Bragg) dynamic hologram. Let us register such a hologram as the interference pattern of the nondistorted plain wave and probe wave with some phase modulation of its wavefront (both waves have the wavelength $\lambda_1$). Let us then reconstruct this hologram at the shifted wavelength $\lambda_2$. In this case we shall obtain the reconstructed probe wave with the phase modulation of its wavefront, equal to that of the primary probe wave, measured in the wavelength of radiation. I.e., the reconstructed probe wave would have the phase modulation of its wavefront, scaled in the ratio $(\lambda_2/\lambda_1)$ with the respect to that of primary probe wave. The use of this feature, in particular, makes it possible to obtain the mutually coherent light beams with the similar, but scaled wavefront distortions, which can be, in turn, used in the above mentioned sophisticated interferometer.

One of variants of the NOF-corrector, using the interferometer with the encoarsed sensitivity and expanded period of output signal modulation, is shown in the Fig.1.2.

In this case the auxiliary laser system has to emit the radiation at two wavelengths $\lambda$ and $\lambda'$; the difference of these wavelengths has to be small: $\Delta\lambda = \lambda - \lambda' = \lambda / m \ll \lambda, \lambda'$; $m \gg 1$. The probe beams at both wavelengths read out the wavefront distortions, imposed by the aberrant beamlet and momentary profile of the corrector. Than the probe beam at the wavelength $\lambda'$ interferes with the coherent nondistorted reference beam in the medium, providing the registration of the thin dynamic hologram. This hologram is read out by another reference beam at the wavelength $\lambda$ and reconstructs the distorted probe beam with the scaled distortions. This beam is combined coaxial with the distorted probe beam at the same wavelength. The intensity

8

in the interference pattern of these two beams varies monotonously from minimum to maximum at the range of phase shifts, imposed by the aberrant beamlet and corrector, m times exceeding that in the usual scheme and thus providing the possibility of their correction.
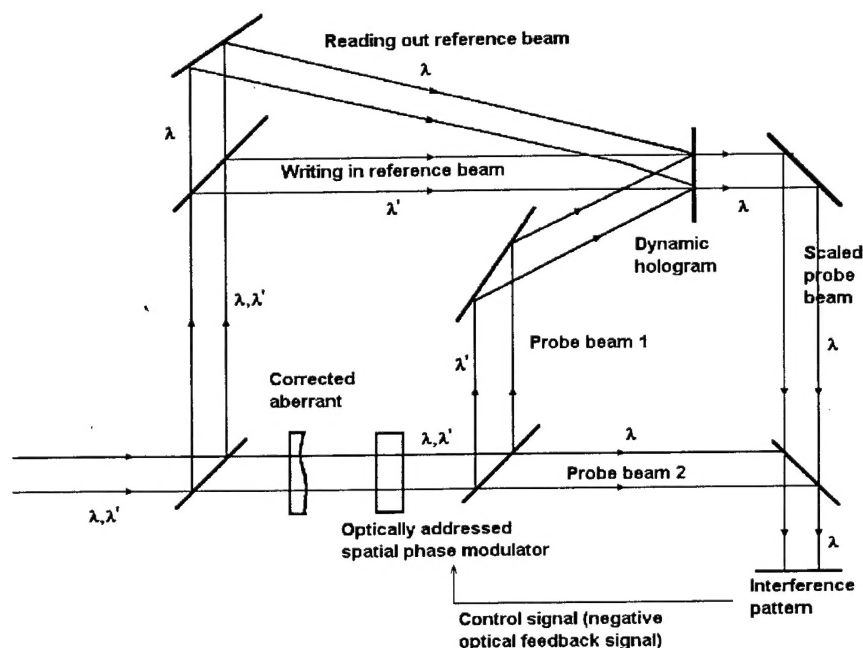


Fig.1.2. The use of interferometer with the encoarsened sensitivity in the scheme of NOF-correction

There are possible other optical schematics, based on the same principles. As to the medium for registration of the thin dynamic hologram, the optically addressed LC SLM, similar to that used as NOF-corrector, seems to be the most promising medium [5].

## 1.2. Problems to be solved or evaluated

The proposed schematics requires experimental feasibility study. In course of this study, which has the preliminary and theoretical character, we shall analyze the existing results in the area, basic problems and approaches to their solution. Further we formulate several problems, which at this moment seem to be the most important and which will be analyzed on the next stages of the work.

As we have said already, there are possible several variants of the interferometer with the reduced sensitivity; one has to choose the optimal.

Even more important seems to be the problem of residual non-corrected error. Similarly to any schematics of stabilization, using the negative feedback, the point of dynamic equilibrium of the system is somewhat shifted with respect to the minimal error signal. In our case it means, that the profile of the dynamic corrector does not completely correspond to the profile of the distortions, imposed by the aberrant beamlet. The magnitude of the residual distortions of the output wavefront, imposed by the summary action of this beamlet and corrector, has to be sufficient for provision of the required distorted profile of the corrector. This problem was not yet analyzed, for the magnitude of the distortions, coped with by the traditional scheme of NOF-correction, was not large and one could neglect these residual error.

Anyhow, there is simple, at least in principle, solution of this problem. One can mount afterwards the first contour of NOF-correction, using the reduced sensitivity interferometer, the second one of the similar schematics or the one, based on the traditional NOF-correction schematics. However, the evaluation of the necessity of such a complication of the system, has to be based on more detailed analysis and numerical simulation.

As to the technological problems in realization of NOF-corrector with the expanded range of corrected magnitudes, the most important seems to be that of fabrication of the "thick" optically addressed LC SLM. The depth of modulation of LC refraction index equals 0.1 - 0.2, so the correction for distortions with the magnitude of dozen wavelength requires the use of LC layer with the thickness of $\sim 10^{-1}$ mm or LC SLM of the sophisticated design. The problem of fabrication of the elements of such a class was already discussed with respect, in particular, of their use as the actuator in the linear adaptive systems [6]. This problem, however, requires much more thorough study, because, in particular, this very element will determine the response time of the overall system.

In addition to shortening the response time, one of the basic problems in design of the "thick" modulators is the problem of fabrication of the elements of the high and reproducible optical quality. Note, that in the case of NOF-correction this factor has much lower importance, for in this case the correcting LC layer is itself introduced into the correction loop.

Rather important from the point of view of extension of the range of magnitudes of the corrected distortions and of the system response time improvement is the proper choice of the pair of auxiliary laser sources and of the medium for the dynamic hologram registration.

Two laser sources are to have the optimal relationship of their wavelengths; in the case of pulse repetitive mode of action the necessary synchronization is to be provided. The interferometric character of the used optical schematics imposes the strict requirements to the modal structure of laser radiation and spatial uniformity of laser beams.

## References

1. Vorontzov M.A., Shmalgauzen V.I. Izvestiya VUZov. Seria Radiofizika, Vol.25, #10, p.1179-1187, in Russian
2. Vorontzov M.A., Kirakosyan M.E., Larichev A.V. Kvantovaya Elektronika, Vol.18, #1, p.117-126, 1991, in Russian
3. Pepper D.M. et al. Innovative adaptive optics and compensated imaging using a liquid crystal light valve. CLEO'93, Technical Digest, paper CThO2, pp.464-466.
4. Warde C., Fisher A.D., Spatial light modulators: applications and functional capabilities. In "Optical Signal Processing", J.L.Homer, ed., Academic Press, NY, 1987, p.477-523.
5. Berenberg V.A., Kamanina N.V., Soms L.N. Holographic correction of distortions using the liquid crystal light modulator for differing frequencies of recording and reading radiation. Izvestiya AN SSSR, Ser.Fizicheskaya, 1991, v.55, #2, p.236-238, in Russian.
6. Onokhov A.P. et al. Optical wavefront corrector based on liquid crystal concept. Proceedings of SPIE, Vol.2201, pp.1020-1026, 1994.

## 2. Nonlinear adaptive systems with the feedback correction for distortions: review

### 2.1. Mathematical model

General schematics of the system for the correction for distortions, implementing the architecture of negative optical feedback (NOF), is based on the NOF loop, necessarily containing the analyzer of the light wave phase, feedback regulator and the corrector, providing phase modulation in accordance with the controlling light field. Most usually the analyzer of the light field phase is based on optical interferometer.

In this case the controlling intensity distribution $I_u(\mathbf{r},t)$ is produced by the interference pattern of the probe wave with the reference one:

$$I_u(\mathbf{r},t) = I_0(\mathbf{r})\,[1+\gamma\cos\delta(\mathbf{r},t)], \tag{1}$$

here $\delta(\mathbf{r},t) = u(\mathbf{r},t) + \varphi_0(\mathbf{r})$ is the phase of output field $A_{out}(\mathbf{r},t)$; $I_0(\mathbf{r})$ - input optical field intensity; $\gamma$ - the rate of interference pattern visuality; $u(\mathbf{r},t)$ - spatial phase modulation, caused by the light interaction with the nonlinear medium; $\varphi_0(\mathbf{r})$ - phase distortions, caused by the optical inhomogeneity in the probe branch of the interferometer.

The nonlinear element imposes the additional phase modulation of the probe wave $u(\mathbf{r},t)$, which is determined by the field intensity in the NOF loop $I_u(\mathbf{r})$:

$$u(\mathbf{r},t) = F\{I_u(\mathbf{r})\}, \tag{2}$$

here $F$ is the operator, describing the response of nonlinear medium (or of the optically addressed phase modulator) to the intensity distribution $I_u(\mathbf{r})$. For the Kerr-like nonlinear media and for some types of SLMs the operator $F$ is linear and thus the equation (2) can be rewritten as the equation, accounting for the finite time of nonlinearity relaxation and for the transverse interaction of diffuse character (excitation diffusion in Kerr-like medium or diffuse washing out of the image in the optically addressed SLM) [1,2]:

$$\tau \partial u / \partial t + u = d\Delta_\perp u + k n_2 l\, I_u(\mathbf{r},t), \tag{3}$$

here $d^*$ is the effective diffusion coefficient, $n_2$ - nonlinearity parameter, $l$ - the thickness of controlling layer, $k = 2\pi/\lambda$ - wave number.

With the account of (1) the equation (3) can be rewritten as follows:

$$\tau \partial u / \partial t + u = d^* \Delta_\perp u + K(\mathbf{r}) [1+\gamma\cos\delta(\mathbf{r},t)], \tag{4}$$

here $K(\mathbf{r}) = kn_2 l \ I_0(\mathbf{r})$ is the function, describing the nonlinear response of the medium, i.e. having the physical sense of the gain in the feedback loop (feedback parameter).

The equation (4) was analyzed in [1]. It was shown that in the stationary state the output field, phase distribution $\delta(\mathbf{r})$ is broken into several domains. In the boundaries of these domains the phase distortions are compensated: $\delta(\mathbf{r},) = u(\mathbf{r},) + \varphi_0(\mathbf{r}) \approx 2\pi n$ ( $n = 0,1, ...$). In the case when $\varphi_0(\mathbf{r}) < 2\pi$, the correction is nearly complete. In the case the diffusion coefficient $d^*$ is to be not more than $1/20 \ x^2$ ($x$ - the diameter of the beam). Enlargement of $d^*$ results in correction fidelity aggravation.

In the Fig.2.1 one can see the stationary dependencies of $\delta(\varphi)$ for various coefficients $K(\mathbf{r}) = K_0$ = const. For $K_0 > 4$ the phase $\varphi$ fluctuations of the input field with the amplitude 0..6 radian are to a large extent dumped. In the Fig.2.2. are shown the calculation results for the model phase distortions $\varphi(\delta) = A| \cos x|, \quad 2\pi \geq x \geq 0$. For $A > 6$ the phase profile $\delta (x)$ of the output field is broken (curve 2, Fig.2.2.). For the sufficiently high values of $K_0 > 8$ the amplitude of phase breaks is close to $2\pi$, reducing hence their influence for the spectral components of the corrected signal with the wavelength, close to that of reference laser, used in the feedback loop.
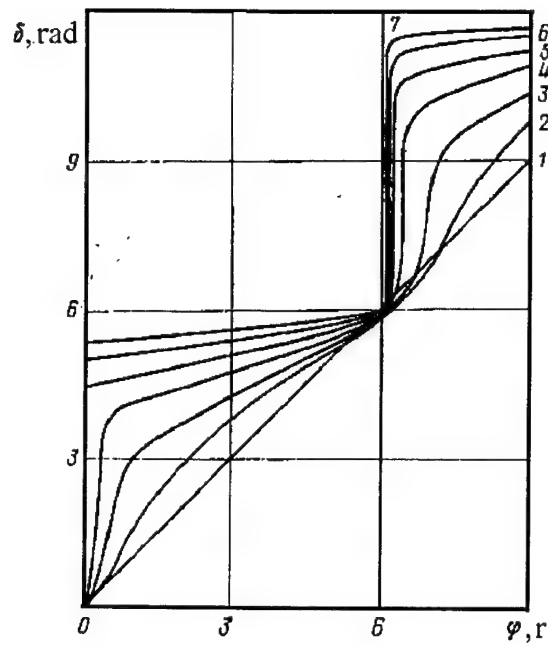
Fig.2.1. The established phase mismatch δ depending on the input field phase distortions amplitude φ for various feedback gain (parameter): 1 - $K_0 = 0$ (feedback is broken), 2 - $K_0 = 0.5$, 3 - $K_0 = 1$, 4 - $K_0 = 2$ , 5 - $K_0 = 4$,  6 - $K_0 = 8$, 7 - $K_0 = 16$
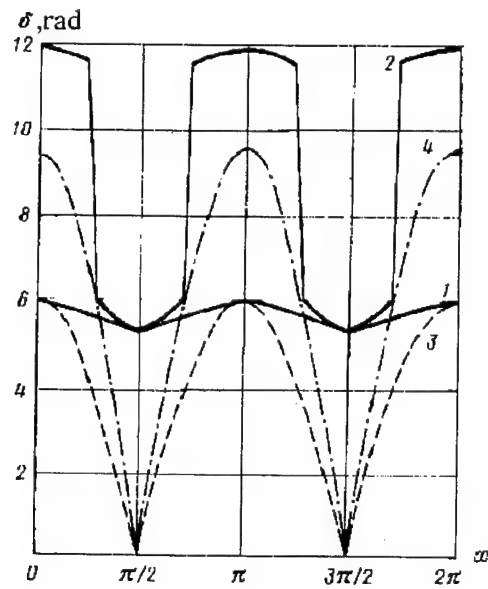


Fig.2.2. The output field phase profile δ(x) (curves 1,2) for various amplitudes of phase distortions φ (x) (corresponding curves 3,4).
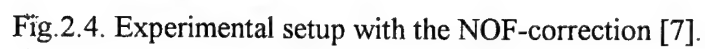
## 2.2. Experimental realization of the NOF correction

First experiments on NOF correction schematics demonstration were done by Fisher and Warde [3,4]. They have used, in particular, the hexagonal matrix of 19 lithium niobate phase modulators, controlled by separate photodiode.

Later most of the activities were done with the liquid crystal spatial light modulators (LC SLM). In such devices the phase retardation of probe radiation is controlled by the intensity distribution of the control radiation on the photoconductor (PC) layer. This distribution corresponds to the interference pattern of the probe wave with the nondistorted reference wave; this interference pattern is delivered to the PC either by TV means or directly by optical relay.

**Systems with TV image relay.** This approach was realized in [5,6]. The experimental setup is shown in the Fig.2.3. It implements the schematics of the modified Twyman-Green interferometer, whose object branch contains the LC SLM. The interference pattern is localized on the fiberoptical plate $S_1$ . The reference wave reaches this registration plane after reflection from the spherical mirror $M_1$. The object (probe) collimated beam with the diameter 15 mm passed through the LC layer, reflected off its dielectric mirror $M_2$, deposed in SLM under the LC layer and once again through LC layer. After it went to registration plane. The interference pattern of two beams was registered by TV camera T. The lens $L_1$ and the TV camera lens provided scaling of the interference pattern image at the control TV tube output, providing its correspondence to the size of primary beam on the SLM. The controlling TV tube with the fiberoptical plate $S_2$ was used for control of LC SLM PC layer.

The system action resulted in enhancement of the interference fringes contrast: after closing the NOF loop the conventional interference pattern was replaced by the set of fringes of practically uniform intensity, separated by narrow dark fringes, i.e. the correction for phase shift inside each fringe was observed.

Fig.2.3. The scheme of the interferometer with the TV NOF.



Fig.2.4. Experimental setup with the NOF-correction [7].

**Systems with optical relay of interference pattern.** Most of the experiments on NOF schematics were carried out in this, seemingly the simplest one, schematics. In the Fig.2.4. is shown the experimental setup, realized in [7]; in [8] another interferometer schematics was used. The beam of radiation of Ar-ion laser with the power ~ 100 mW was expanded up to the diameter of 10 mm and reached the interferometer, comprised by the dielectric mirror of LC SLM and edge between glass substratum and LC layer. The latter layer provided the phase modulation. Light protective layer, placed between PC and dielectric mirror, practically excluded influence of the object (probe) wave onto PC layer from inside the interferometer.

The probe and reference waves, reflected by the interferometer, entered the feedback loop. The Fourier filter (lenses L1 and L2 and the pinhole in the focal plane) provided elimination of noise of higher spatial frequencies; the cleaned off interference pattern via optical fiber twist reached the PC layer of SLM.

Model distortions were introduced by auxiliary illumination of the SLM PC layer; the uniform illumination provided the control of stationary phase retardation in the system.

In the Fig.2.5a is shown the system output in the absence of feedback, when the pinhole D was closed. The phase modulation, introduced in the plane of SLM reveals itself in the amplitude modulation, caused by diffraction (the distance from the lens L2 to the input of fiberoptical twist was about 2 m, while the beam diameter was 10 mm. Opening of pinhole D led to establishment of homogeneous intensity distribution at the system output (Fog.2.5b) - the evidence of correction for phase distortions.

In the case of elimination of this pinhole the high spatial frequency noise resulted in diffractive remixture of the light and thus in instable behavior of the system (see further).

In [7,8] there was demonstrated the correction for phase distortions with the magnitude of not more than $2\pi$. However, for the higher magnitudes the situation is much worse. It was analyzed in [8]. The object branch of the interferometer contained the distorter (window glass). In the absence of NOF-loop the output interference pattern revealed several fringes. After NOF-loop closure several edges of piston-like

17

changing of wavefront phase were observed across the beam section; these edges revealed movement and instable behavior. Each domain revealed practically uniform phase distribution, differing in $2\pi$ with respect to the neighboring domains. Some domains gradually disappeared, while other grew in time. For the characteristic response time of SLM in 10 ms the transient period of system behavior took some 0.5 seconds; however, the final stable distribution lacked complete correction for phase distortions.

Pepper et al. [9] have demonstrated the possibility to apply the LC SLM in NOF-loop for correction for static and dynamic distortions. In these experiment the optical relay of three lenses was used in NOF-loop; NOF correction provided correction for distortions, imposed by etched glass plate, improving the Sterol ratio from 0.017 to 0.82.

On the next stage of this experiment [9] the correction was demonstrated for image of incoherent object. The standard US AF test-object, illuminated by tungsten lamp was imaged in the schematics, shown in the Fig.2.6. The radiation of the auxiliary referent laser passed through the distorting layer and through the actuating part of SLM; then it entered the NOF-loop, where it interfered with the nondistorted wave of the same laser radiation.

The wide spectral band (width ~ 200 nm, limited just by parameters of optical elements, used in the experiment) radiation from the imaged test object passed via the same distorting path; the action of LC SLM resulted in significant improvement of the image quality. In the absence of NOF-correction the spatial resolution of model system was ~ 5 diffraction limited values with the distorting element and ~ 1.25 DL without; the NOF-correction provided its improvement up to 1.4 DL.
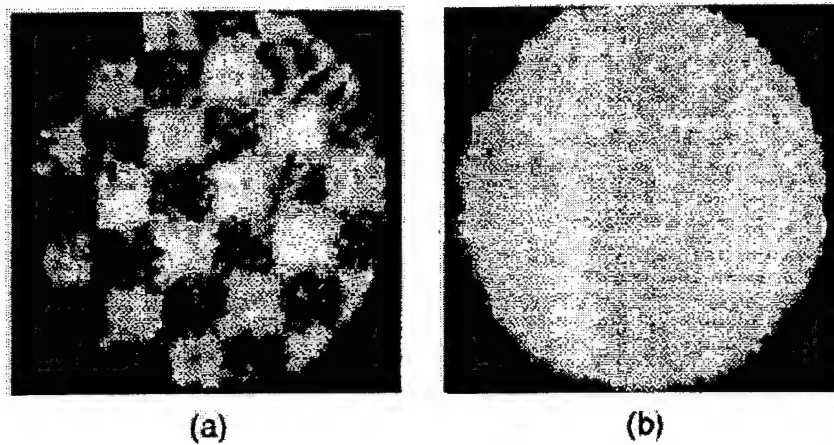
Fig.2.5. Intensity distribution in the output plane without (a) and with (b) NOF-
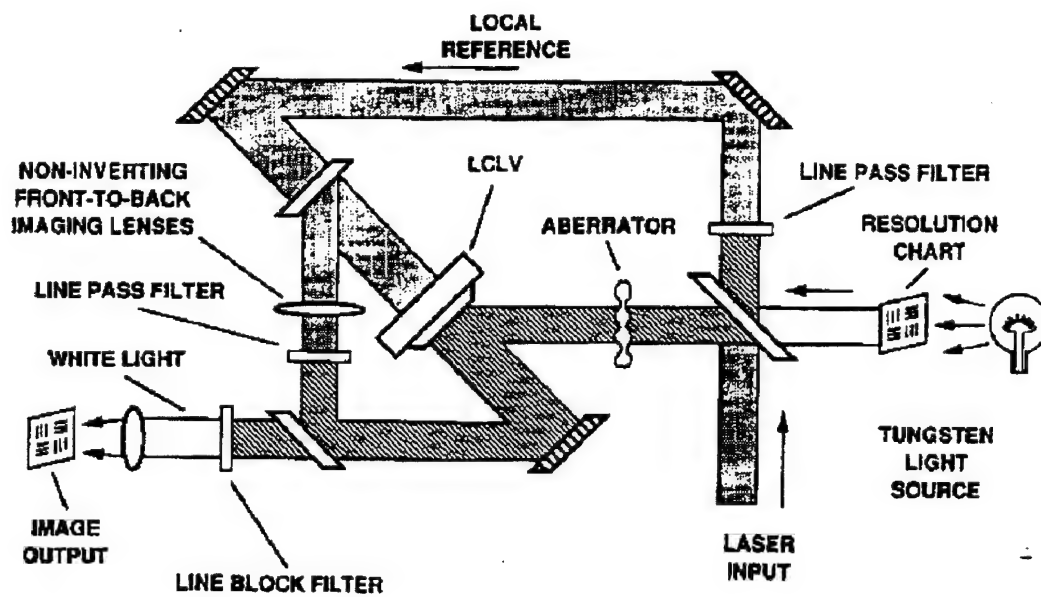
correction.



Fig.2.6. Experimental setup with the NOF-correction [9]..

## 2.3. Instability of spatial structure of light field in 2D NOF system

In the system with 2D optical feedback there take place the problems, which are quite novel for the optics, related to the spatio-temporal stability of the processes of light field formation. Spatio-temporal changes in the field structure in NOF-loop can result in generation of the complicated spatial structures.

Usual optical instabilities (say, generation in laser cavity) are caused by the passing of some threshold value by the feedback rate and reveal usually only time dependencies. 2D NOF schematics reveals also the quite novel spatial effects, which do not have analogies in optics. It is caused by the mutual coupling of various points of beam section, resulting of the diffraction and non-local character of nonlinear process involved. In our case these are first of all the diffraction mixing of radiation in optical contour of the feedback loop and diffusion of charge carriers across the photoconductor of LC SLM.

These effects were studied in the experiments [10,11,12]. The experimental setup is shown in the Fig.2.7. The beam splitter M1 (or edge glass substratum - LC layer in SLM) and dielectric mirror of the SLM M2 worked together as the Fizot interferometer.

The interfering waves reflected off the beam splitter M3 and entered the feedback loop contour, made by the mirrors M4-M6, lenses L1 and L2 and Dovet prism. The polaroid P provided variation of the light intensity in the feedback contour and thus of the feedback rate K. The Dovet prism rotated the image in arbitrary angle; mutual movement of lenses provided variation of the image scale. The aperture D between the lenses provided the control over the diffraction mixing rate. Two SLMs (spatial resolution 2 and 10 lines per millimeter) were used in the experiment.

The following dynamic processes were observed:

1. Rotational instability, resulting of field rotation around the axis of optical system in the feedback loop. Such a rotation can be the result of either insufficiently good adjustment of optical elements or tilt of TV monitor. In the Fig.2.8 one can see the multi-sheet structures, which are caused by the field rotation in feedback loop. Changing of this rotation angle resulted in changing of the structure rotation speed; for some angles the structures were stable and did not rotate.

Spatial structures, speed and direction of rotation were determined by the SLM spatial resolution and by the influence of diffraction mixing.

2. The shear instability. The linear shift of the image results in various autowave processes. The typical kind of such a wave is shown in the Fig.2.9. These structures were greatly influenced by the distortions in the beam path. For large image shifts (>1/4) the shear structure was stable. Increasing of spatial mixing in NOF-loop resulted in larger spatial period and lower movement velocity of autowaves.

3. Optical spirals. Image scaling and rotation resulted in spiral-shaped structures (Fig.2.10). The direction and speed of rotation of spirals as well as number of branches depended on the angle of image rotation, by scaling magnification and by light intensity in NOF-loop.

4. Optical turbulence. The increase of feedback parameter (gain) K, i.e. of the field in the feedback loop intensity, results in decay of spirals and of the multi-sheet structures (Fig.2.11). Increase of K results first in the structures' decay at the beam periphery; separate fragments of the structure start independent behavior. Growth of K results in increase of this area.
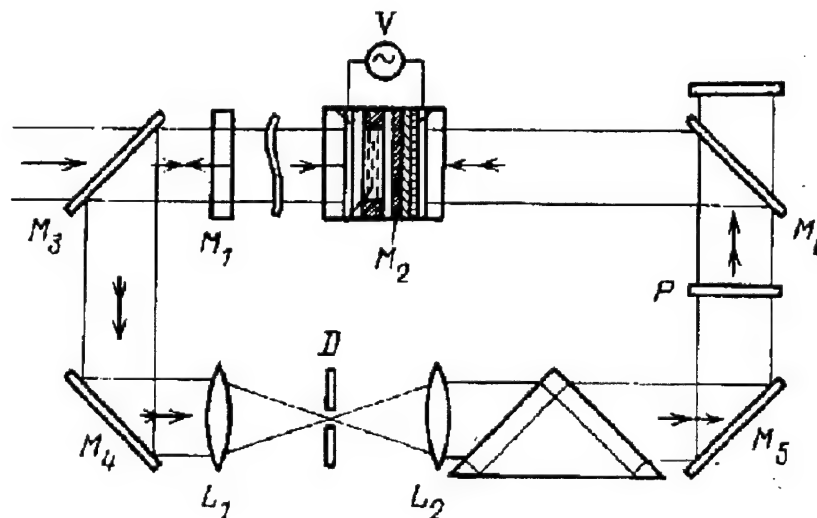


Fig.2.7. Experimental setup for studying of the instability of spatial structure of the beam in the system with feedback .
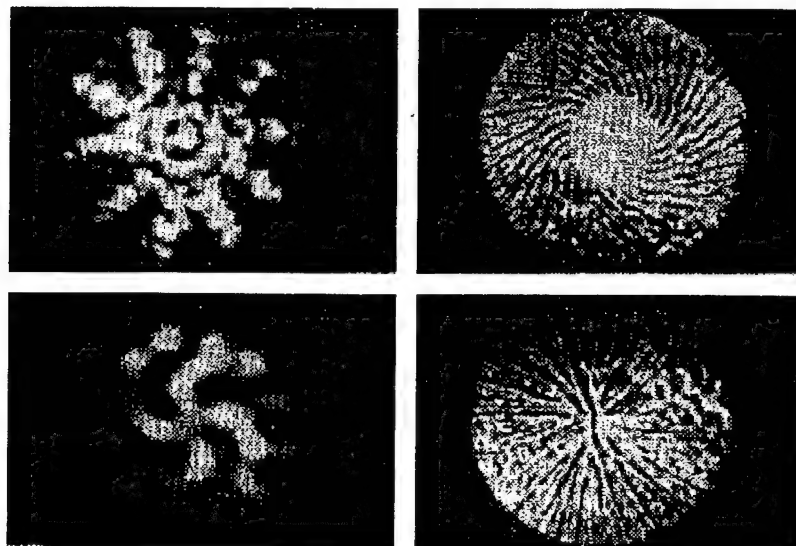
Fig.2.8. Various kinds of rotational instability.
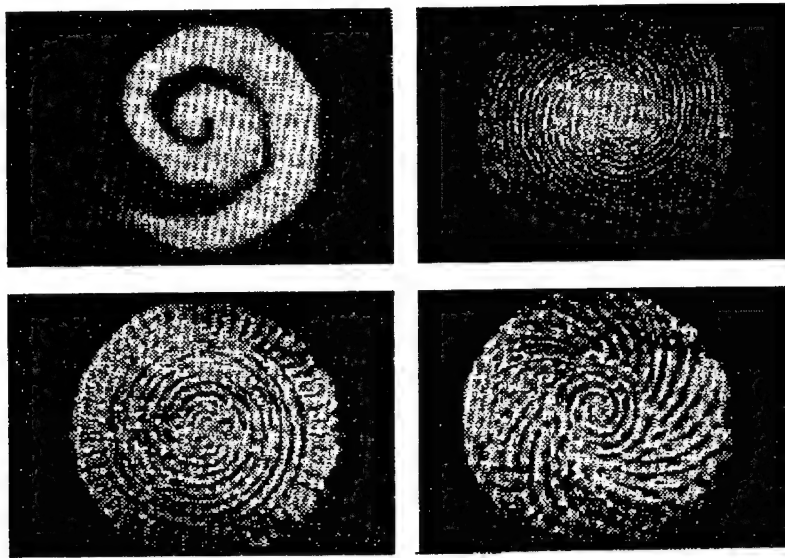


Fig.2.9. Shear instability.

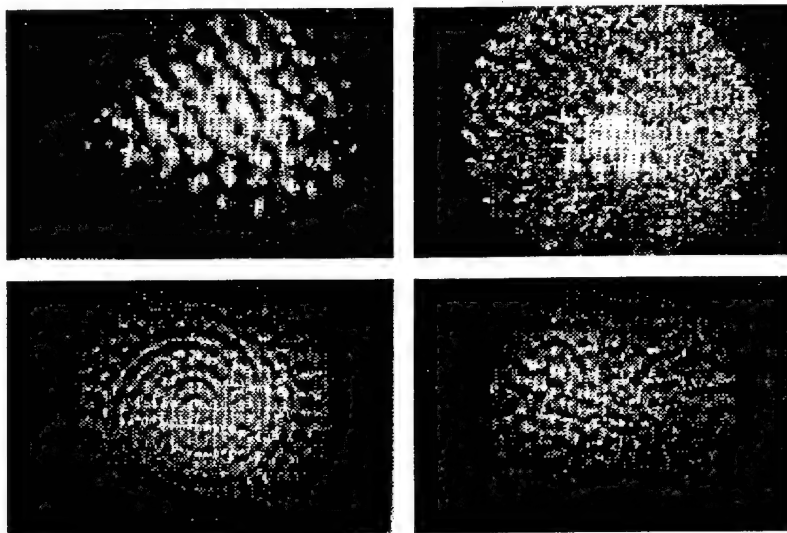Fig.2.10. Spatial structure instability, caused by image rotation and scaling.



Fig.2.11. Light field stokhastization.

# References

1. M.A.Vorontsov, A.V.Koryabin, V.I.Shmalgauzen. Controlled optical systems. Moscow, "Nauka", 1989 (in Russian)
2. Ch.Gibbs. Optical Bistability Moscow, 1988 (Russian edition)
3. A.D.Fisher and C. Warde, Opt. Lett., 4, 131-133 (1979).
4. A.D.Fisher and C. Warde, Opt. Lett., 8, 353-355 (1983).
5. M.A.Vorontsov, AF.Naumov. Preprint, Physical Faculty of Moscow State University, #34, 1987.
6. M.A. Vorontsov, V.A. Katulin, A.F. Naumov, Opt. Commun., 71, 35-38 (1989).
7. E.V. Degtiarev and M.A. Vorontsov, J. Opt. Soc. Am. , B/Vol. 12, No. 7, 1238- 1248 (1995).
8. M.A.Vorontsov, M.E.Kiracosyan, A.V.Larichev, Kvantovaya Elektronika, 18, #1, p.117-120 (1991, in Russian)
9. D.M. Pepper, P.V. Mitchel, C.J. Gaeta, M.L.Minden, W. P.Brown, T.R. O'Meara and U. Efron, Innovative adaptive optics and compensated imaging using a liquid crystal light valve, in Conference on Lasers and Electro-optics, Baltimore, MD (1993).
10. S.A.Akhmanov, M.A.Vorontsov, D.V.Pruidze, V.I.Shmalgauzen. Izvestiya AN SSSR, Ser.Fizicheskaya, 52, #2, p.374 (1988, in Russian).
11. M.A.Vorontsov, Yu.D.Dumarevsky, D.V.Pruidze, V.I.Shmalgauzen. Izvestiya AN SSSR, Ser.Fizicheskaya, 52, #2, p.354 (1988, in Russian).
12. S.A.Akhmanov, M.A.Vorontsov, V.Yu.Ivanov. Pisma v JETF, #12 (1988, in Russian).

## 3. *Technology problems, related to NOF-correction with holographic converter*

The approach under discussion in this Report is based, in particular, on the use of two key optical elements: the optically addressed liquid crystal spatial light modulator, OA LC SLM, providing the deep phase modulation of the wavefront, and the element of similar design, which can be used for recording of the thin (plain) dynamic holograms. The corresponding problems are discussed in this Chapter.

### 3.1. OA LC SLM with the large depth of phase modulation

The characteristics (both realized, and potentially possible) are considered of optically addressed liquid crystal spatial light modulators of (OA LC SLMs), ensuring large (about several or several dozen $\pi$) depth of phase modulation. The large depth of phase modulation requirement is key for OA SLMs in the suggested scheme of correction for distortions of optical systems. The second on the importance is the opportunity of OA SLMs operation at repetition rates from units up to dozens and hundreds Hertz. These requirements cannot be executed on a maximum simultaneously. In each particular case the search of compromise variant of SLM design is necessary.

It is obvious beforehand that, for the achievement of demanded depth of phase modulation, there are necessary rather thick (about ten micron) LC layers. In this connection, apparently, only nematic LC can be used, as far as the creation of thick layers of chiral smectic LC (ferroelectric LC, FLC) is not available. Further, if it is not stipulated especially, it will be assumed that the S-effect in nematic LC is used for phase modulation.

**Estimation of LC SLM phase shift and refresh time**

At the use of S-effect for light modulation, the phase shift $\Delta\Phi$ between ordinary and extraordinary rays is defined as:

$$\Delta\Phi = \frac{2\pi}{\lambda} \int_0^L [n(z) - n_\perp] dz, \tag{1}$$

Here L - thickness of a LC layer, n (z) - distribution of a refraction index for extraordinary beam along LC layer, $n_\perp$ - refraction index for ordinary beam, $\lambda$ - wave length.

The maximal possible value of phase shift $\Delta\Phi$, as appears from equation (1), can be estimated as

$$\Delta\Phi_{max} = 2\pi\Delta nL/\lambda, \tag{2}$$

Here $\Delta n$ is the optical anisotropy of LC.

It should be noted that in practice the maximum achievable value of size $\Delta\Phi$ always is less then $\Delta\Phi_{max}$. This circumstance is connected with the fact that the initial orientation of the director, as a rule, differs from the planar, and the values $\Delta\Phi$ close to $\Delta\Phi_{max}$ are achieved at a sufficient (more than 6-7 times) excess of a voltage U on a LC layer above threshold value $U_S$.

The potentially possible meanings of SLM refresh time are determined by switch-in $\tau_{in}$ and switch-off $\tau_{sw}$ time of S-effect. An opportunity to not take into account, at refresh time estimations, the contribution of photoconductor response dynamics is caused by relatively low requirements to SLM resolution (units lp/mm). It allows to use high-speed photoconductors, with the response time essentially less than that for nematic LC.

The times $\tau_{in}$ and $\tau_{sw}$ at small director tilt angles are determined as

$$\tau_{in} = \frac{\gamma_1 L^2}{\Delta\varepsilon\varepsilon_0 U^2 - \pi^2 k_{11}}, \quad \tau_{sw} = \frac{\gamma_1 L^2}{\pi^2 k_{11}}, \tag{3}$$

Here $\gamma_1$, $k_{11}$ – the factors of viscosity and elasticity, correspondingly, $\varepsilon_0$ – dielectric permeability of vacuum.

At room temperature the typical size of factors of viscosity and elasticity has the following values: $\gamma_1 \sim 5\times10^{-2}$ kg/m x s, $k_{11} \sim 10^{-11}$ N. For L=10 μm, the maximal possible reversibility is, according to the formulae (3), about 20 Hz. The similar reversibility values are really observed for SLMs powered by alternating voltage. For dc-powered SLMs the reversibility is essentially lower (units of Hertz). This drop is connected with the dc-current polarization in the structure "photoconductor – LC" (PC-LC)

## DC-Powered SLMs with Photoconductor - Liquid Crystal Structures

Apparently, for the first time the phase modulation of light in PC-LC structure was studied in [1], where solid solutions of CdS and ZnS (composition $Zn_{0.7}Cd_{0.3}S$ with $\lambda_{max} = 0.442$ μm) were used as photoconductors. The phase modulation depth reached $\pi$ at the wave length of reading radiation 0.633 μm. The disadvantage of solid

26

solutions Zn-Cd-S is the high level of spatial noise caused by non-uniform distribution of the co-dopants Cu and Cl that are admixed to increase the sensitivity of structure.

A number of other photosensitive structures were investigated as photocondutors in transmission-type SLMs. In particular, $As_{10}Se_{90}$, that is transparent for reading light wavelength of more than 0.6 μm [2]; the amorphous silicon [3], having wide area of spectral sensitivity (0.5 - 1.5 μm); polymer photoconductors [4] on a basis of sensitized poliimides, having the greatest resolution (23 % is achieved at 120 lp/mm), but the small reversibility (lower then 1 Hz). All these structures, working at dc-power in transparent mode, require the reading radiation not influencing essentially the photoconductor layer. This leads to the limitation in the image brightness increase to only $10^2$ - $10^3$. The response time of the structure is determined by charge relaxation processes on PC-LC boundary, and it is almost independent on thickness of a LC layer, and is within several tenth - several units of seconds.

The phase modulation depth can be increased approximately 2 times in SLM operating in the reflective mode, rather then in the transparent.

Two configurations of reflective SLMs are known differing by the position of the reflecting mirror. For the first type, both the photoconductor and LC are a the same side towards the mirror. For example, in [5,6] the multi-layer dielectric mirror was deposed on a surface of an optical fiber plate, and then was covered by the layers of a transparent conducting electrode, and photoconductor ($As_{10}Se_{90}$ or ZnSe). For the latter case, the phase shift ~ $6\pi$ was realized for reading wavelength 0.633μm at change of the writing light intensity from $10^{-7}$ W/cm$^2$ up to $10^{-4}$ W/cm$^2$, at the reversibility about 1 Hz [6].

For the second type, the mirror separates photoconductor from LC. In order to provide SLM operation at the constant voltage, as a rule, a mosaic metal (Al) mirror is used. The SLM resolution is determined by the sizes of the mirror element. The resolution ~40 lp/mm is obtained at the gap between elements ~2 μm. Such mirror allows reading in wide spectral area. However its reflection coefficient usually does not exceed 90%. In comparison with SLMs of the first type the intensity of reading light can be increased approximately on the order. Estimations show that SLM with a similar mirror and ZnSe photoconductor with thickness 2 - 4 μm and LC layer ~10 μm can provide

the modulation depth of reading light in a wide spectral range up to $10\pi$ at reversibility ~1 Hz.

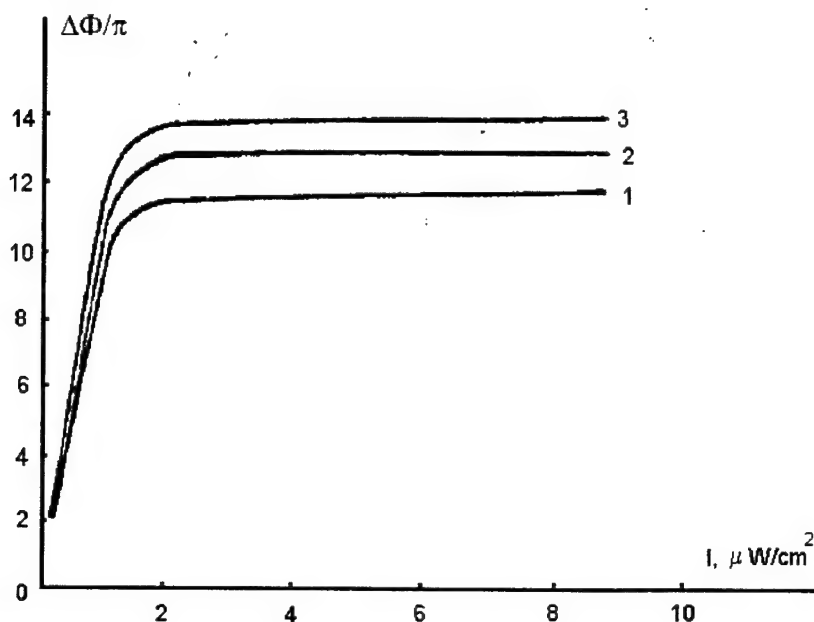Here are some examples of dc-powered SLMs:



Fig.3.1. Phase modulation (wavelength 442 nm) dependence vs. intensity of control radiation . Voltage at the cell: 1 – 9.72 V, 2 – 10.8 V, 3 – 11.88 V.

a) The dependence of phase modulation depth of in PC-LC structure on the intensity of writing light and driving voltage is given in Fig.3.1, reading light wavelength 0.442 μm [7]. The photoconductor ($Zn_{0.8}Cd_{0.2}S$) thickness was equal 1.5 μm. The SLM switch-off time was ~2 s at the LC thickness 10 μm. There were no data on the LC optical anisotropy values in this work. Assuming $\Delta n$=0.2, the limiting value of phase shift $\Delta\Phi$ cannot surpass $9\pi$, so the value $8\pi$ given in the article is quite real.
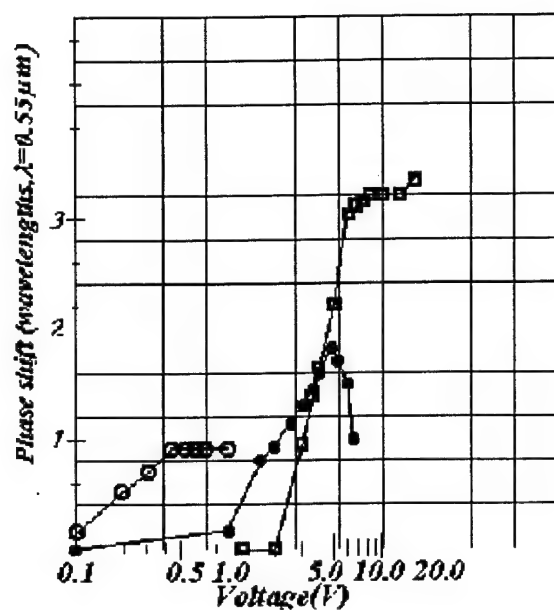
Fig.3.2. Experimentally measured phase shift on double pass through the SLM vs. applied voltage; Δn≈0,16; rings correspond to LC thickness of 5 μm (two specimens with different properties of ZnSE layer), empty squares correspond to the LC thickness of 10 μm.
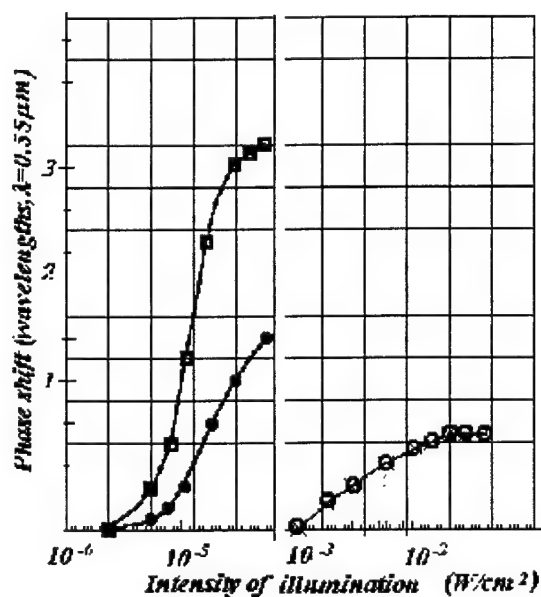


Fig.3.3. Experimentally measured phase shift on double pass through the SLM vs. intensity of controlling radiation; Δn≈0,16; rings correspond to LC thickness of 5 μm (two specimens with different sensitivity of ZnSE layer), empty squares correspond to the LC thickness of 10 μm.

29

b) The dependence of phase shift on the driving voltage and on the intensity of writing light at optimum powering voltage are given in Fig.3.2 and Fig.3.3 for structure ZnSe - LC at photoconductor ~2 μm and LC thickness 10 μm. The measurements were carried out at the white light reading in shift interferometer. The SLM operated at repetition rate 1 Hz [8].

The choice of an optimum powering voltage for the given PC-LC structure is of the primary importance to obtain the maximal $\Delta\Phi$. For a particular PC-LC structure, this maximal value is determined by the following factors:

- Dark voltage applying to LC should not exceed threshold value $U_S$ (usually 0,5 -1V), so that the resulting $\Delta\Phi$ would determined extremely by the writing radiation.

- The photoconductor layers, irrespective to deposition technology, should keep their optical quality (uniformity, low scattering, porosity etc.) at thickness 2 - 4 μm, and should have the dark specific resistance $10^{12}$ - $10^{13}$ Ω x cm, and the specific resistance under illumination $10^9$ Ω x cm.

- The LC specific resistance should be about ~$2\times10^{11}$ Ω x cm at the LC layer saturation voltage ~15V at the LC layer thickness 10μm.

For the given set of parameters the calculated optimal driving voltage at SLM is ~10V, for $U_S \approx 1V$, that coincides with the experimental value. According to formula (2), the calculated phase shift $\Delta\Phi_{max}$ amounts $6\pi$, i.e. 1.5 times more then in experiment. The reasons to that were specified above. It was confirmed by the measurements of SLM modulation characteristic in crossed polarizers.

The given examples testify to the opportunity of creation OA LC SLMs providing phase shift in white light up to $6\pi$-$10\pi$ for transparent SLMs, and double value - for reflecting SLMs. The basic lack of dc-powered SLMs is low reversibility (units of Hertz). This imperfection is caused by transient effects on the border photoconductor – liquid crystal, because of current polarization effects.

**AC-Powered SLMs with Photoconductor - Liquid Crystal Structures**

It is possible to increase SLMs reversibility up to the limiting meanings determined by relations (3), using alternating voltage powered SLMs. Here an opportunity opens of SLMs manufacturing with a solid mirror and with a blocking

layer separating LC from photoconductor. Except the phase shift increase, this allows to raise the intensity of reading radiation in comparison with dc-powered SLMs.

The problems of SLMs optimization are discussed in [10-13]. The photosensitive heterostructure representing the photo diode working in a mode of photoinduced carriers accumulation is examined in [11,12]. Basically the factors determining sensitivity of structures are analyzed which are reduced to the following:

- The reduction of thickness of LC and dielectric layers and the increase of their dielectric permeability;
- The photoconductor layer thickness and dark resistance increase and reduction of its dielectric permeability;
- Increase of driving voltage;
- Increase of the modulation characteristic slope and threshold by the choice of electrooptical effect in LC.

It shall be noted that some of the listed factors interfere with increase of phase shift.

Apparently, the greatest phase shifts were realized in SLMs with Zn-Cd-S photoconductor described in work [10]. The calculated and experimental modulation characteristics are given in Fig.3.4. The thickness of photoconductor amounts 4.5 μm, and LC - 5μm. The dependencies are given for four various LC compositions differing by dielectric permeability. The modulation characteristic is given in Fig.3.5 depending on intensity of writing light intensity at various SLM driving voltage.

It is necessary to note that ac-powered SLMs use a wide nomenclature of photoconductors: monocrystal [14], amorphous and polycrystalline [15,16], metal-dielectric-semiconductor structures [17]. The last structures do not allow to receive large phase shifts, but they have a rather high spatial resolution and speed. Let's note some features of SLM characteristics with the most usual photoconductors.
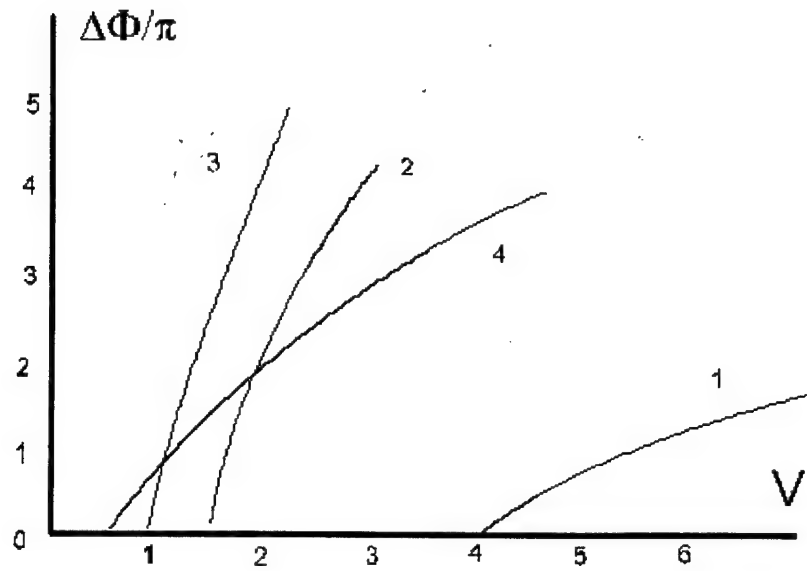
Fig.3.4. Modulation vs. applied voltage via S-effect in LC of various composition with
the thickness of 5 μm.



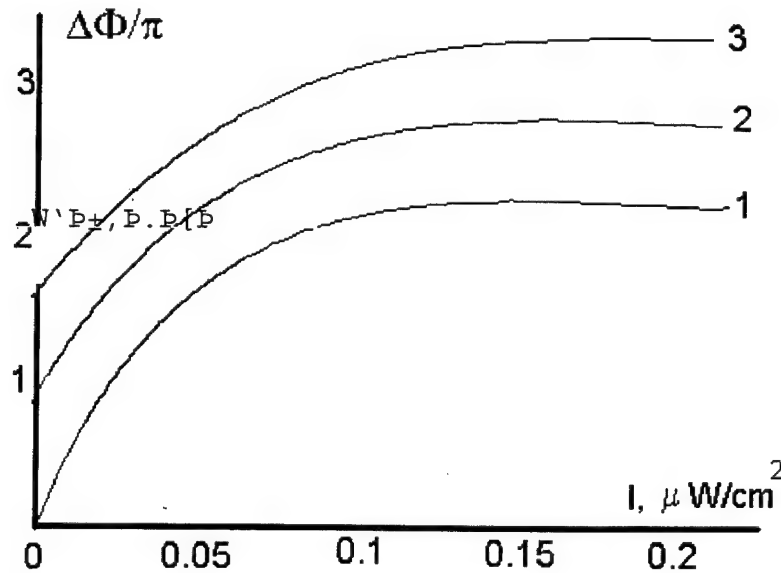Fig.3.5. Phase shift dependence vs. control radiation intensity for the structure of
$Zn_{0.7}Cd_{0.3}S$ (PC), 45 mm thickness and NLC, 5 μm thickness (curve 2 in the Fig.3.4),
S-effect, f=100 Hz, feeding voltage (1) – 3.2 V, (2) – 3.6 V, (3) – 4 V.

The polycrystalline silicon photoconductors , because of small absorption have large thickness (~100μm); this, together with high (~1300 cm$^2$/V x s) mobility of carriers, provide the low spatial resolution. The last can be eliminated by the formation a p-n barrier on the PC-LC border [18]. Thus the resolution is increased from units up to several tens lp/mm.

The photoconductors using GaAs monocrystal [19] or Bismuth silicate $Bi_{12}SiO_{20}$ [20] have the thickness 0,5 and 2 mm, correspondingly, and, as a consequence, the low spatial resolution and high level of spatial noise. The best characteristics are provided with structure CdS-CdTe [21] at CdS thickness 19-20 μm.

In summary we shall note, that the greatest depth of phase modulation in white light (~4π) at a rather high reversibility (~10 Hz) was realized in works [22,23] for SLMs with the GaAs monocrystal photoconductor with 50-100 μm thickness (similar SLM is described also in work [24]). The basic imperfections of these SLMs are their initial phase heterogeneity and the rather high level of spatial noise.

**Conclusion**

The basic conclusion from the review is as follows. The most perspective OA LC SLMs providing the large phase shifts at a relatively high reversibility are the SLMs with dielectric mirror working at a alternating driving voltage. The opportunity of realization of potential opportunities for such SLMs requires a careful matching of photoconductor ans LC parameters, the optimization of the driving voltage amplitude and frequency, and the high quality of dielectric mirror deposited on the photoconductor.

## 3.2. Optically addressed liquid crystal spatial light modulators for dynamic holography

Another key technology to be used in the system discussed is that of recording of the plain dynamic hologram. In fact this technology has very much in common with the technology of holographic correction for distortions, but in our case the plain (thin) character of the hologram to be used is the main specific feature of this element. At the same time it plays only the auxiliary role - the hologram is used only for conversion of the auxiliary laser radiation, but it does not deal with the signal, processed by the overall system with correction for distortions; so, the diffraction efficiency of this

element is not such an important factor, as in the case of similar element use for correction for distortions. At this moment, seemingly, the only available elaborated medium for the plain dynamic hologram record is to be based on the same technique of the optically addressed liquid crystal spatial light modulators (OA LC SLM). The technology of such elements and their application for correction for distortions are the subject of the special study, accompanying this one according to the Contract #F6170896W0318, concluded by EOARD, US AF, USA and Company LOS Ltd., St.-Petersburg, Russia. So in this report we should only in brief outline the most important features.

The OA LC SLM [25-30], which are widely used for recording of the dynamic holographic gratings, are comprised by the multi-layer structure, mounted between two electrodes, at least one of which is transparent [10]. One of the layers of SLM is made of photoconductor (PC) and another of liquid crystal (LC). Most usually the light modulation is produced by means of modulation of LC birefringence or optical activity: local variation of PC parameters results in corresponding variation of the voltage on LC and in its molecules rotation.

The possibility to vary in wide range the physical and chemical parameters of LC [31] and to use various PC [10] provides significant possibilities of LC SLM parameters, such as spectral range and sensitivity, response time and reversibility, resolution etc. variation.

Phase modulation can be produced both by nematic LC (NLC) and smectic LC (SLC). Up to day two of numerous polymorphous modifications of SLC are practically used: the ferroelectric chiral $C^*$ phase ($SmC^*$) and chiral $A^*$ ($SmA^*$) phase.

In the case of NLC the light modulation is produced via the controlled birefringence (S- and B-effects) or twist-effect [32]. In SLM with $SmC^*$ LC light is modulated by Clark - Lagerwall [33] or DHF-effects [34]. In the case of SLM with $SmA^*$ LC the light is modulated by the electroclinic effect [35]. Both inorganic (crystalline, polycrystalline and amorphous) [10] and organic [30] photo semiconductors can be used as the PC in SLM. So the parameters of OA LC SLM can be varied in approximately the following ranges:

| | |
|---|---|
| Spectral sensitivity range, μm | 0.3..1.1 |
| Sensitivity: | |

|                          |                |
|--------------------------|----------------|
| energy, $\mu J/cm^2$      | 0.001..400     |
| power, $\mu W/cm^2$       | 0.5..1000      |
| Resolution, lp/mm        | up to 400..600 |
| Diffraction efficiency, % | up to 30..40   |
| Frame repetition rate, Hz | up to 1000     |
| Feeding voltage, V       | 10..100        |

Obviously, the whole set of best parameters is not available in one and the same kind of SLM. As we have said already, in our case the diffraction efficiency, as well as energy and power sensitivity and spectral range are not the critical parameter, so one can choose the elements with highest repetition rate, improving thus the overall response time of the system. In this case the best parameters are demonstrated by the elements, based on ferroelectric LC; in Fig.3.6 illustrates the response properties of one of such elements, realized in Vavilov State Optical Institute [8].
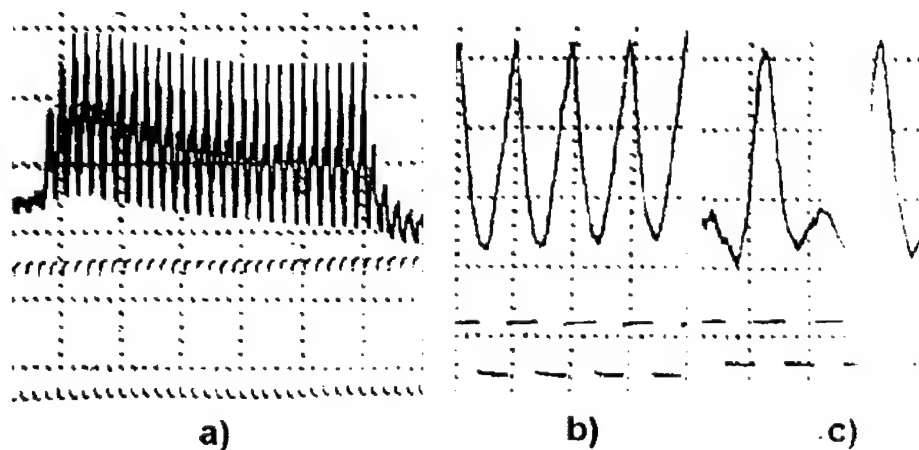


a)  b)  c)

Fig.3.6. Diffraction to the first order on dynamic hologram, using ferroelectric LC + $\alpha$-SiH PC; feeding voltage repetition rate 1 kHz: (a) single light pulse with duration of 23 ms; (b) and (c) – pulses with repetition rate 1 kHz and 500 Hz

# References

1. A.Vasiliev, Trudy FIAN (Proc. Of Lebedev Phys. Inst), 1981, v. 126, pp. 3-75
2. F.Vladimirov et al, Optiko-Mekhanicheskaya Prom. 1985, № 5, pp. 1-3.
3. L.Samuelson, H. Wieder, G. R. Guarnieri et al. Áppl. Phys. Lett., 1979, vol. 34, No.7, p.450-452.
4. V.Myl'nikov ey al, ZHTPh letters 1985, т. 11, № 1, pp. 38-41.
5. N.Pletneva et al, Kvantovaya elektron., 1983, т. 10, № 9, pp. 1892-1895.
6. B.Aleksandrov et al, Opticheskiy Zhurnal, 1997, № 4, pp. 94-96.
7. A.Vasiliev, PhD Thesis, Moscow, Lebedev Phys. Inst., 1980.
8. A.Onokhov, A.Seregin, private communication
9. P.Kotler, Avtometriya 1976, № 6, pp. 65-69.
10. A.Vasiliev, D.Cassasent et al., Spatial Light Modulators, Moscow, 1987, 320 pp.
11. L. M. Fraas, J. Grinberg et al. J. Appl. Phys., 1976, vol. 47, No. 2, p. 576-583.
12. L. M. Fraas et al. J. Appl. Phys., 1976, vol. 47, No. 2, p. 584-590.
13. J. D. Michaelson. Proc. SPIE, 1980, vol. 218, p. 88-95.
14. K. Sayyah et al. Appl. Opt., 1989, vol. 28, p. 4748-4756.
15. I. Abdulhalim, G. G. Moddel, K. M. Jonson. Appl. Phys. Lett., 1989, vol. 55, p. 1603-1605.
16. G. G. Moddel et al. Appl. Phys. Lett., 1989, vol. 55, p. 537-539.
17. T. Harikawa et al. Mat. Res. Soc. Symp. Proc., 1991, vol. 219, p. 203-208.
18. U. Efron et al. J. Appl. Phys., 1985, vol. 57, p. 1356-1368.
19. D. Armitage et al. Appl. Opt., 1989, vol. 28, p. 4763-4771.
20. P. Aubourg et al. Appl. Opt., 1982, vol. 21, p. 3706-3712.
21. W. P. Bleha et al. Opt. Eng., 1978, vol. 17, p. 371-384.
22. M. A. Vorontsov et al. Opt. Eng., 1995, vol. 34, No. 11, p. 3229-3239.
23. M. A. Vorontsov et al. J. Opt. Soc. Am. A, 1996, vol. 13, No. 7.
24. Yu.Dumarevskiy et al., Optiko-Mekhanicheskaya Prom., 1989, № 12, pp. 9-11.
25. O.V.Garibyan, I.N.Kompanets, A.V.Parfyonov et al, Opt.Commun. 1981, Vol. 38, No. 1, p. 67-70
26. E. Marom, U. Efron, Opt. Lett. 1987, Vol.12, No. 7, p. 504-506
27. N.V.Kamanina, L.N.Soms, A.A Tarasov, Opt. Spektrosk., 1990, Vol. 68, No. 3, p. 691-693, (rus)
28. K. M. Johnson, C. C. Mao, G. Moddel, M. A. Handschy, K. Arnett, Opt. Lett. 1990, Vol. 15, No.20, p. 1114-1116
29. S. Fukushima, T. Kurokawa, M. Ohno, Appl. Phys. Lett. 1991, Vol. 58, No. 8, p. 787-789
30. V. S. Myl'nikov, Optik. Zh., 1993, No. 7, p. 41-45, (rus)
31. I.F.Grebyonkin, A.V.Ivashenko. Liquid crystal materials. Moscow, Himiya, 1989, 288 pp.
32. V. G. Chigrinov. Kristallografiya, 1982, Vol. 7, No. 2, p. 404-430, (rus)
33. N. A. Clark, S. T. Lagerwall, Appl. Phys. Lett. 1980, Vol. 36, No. 11, p. 899-901
34. L. A. Beresnev, L. M. Blinov, D. I. Dergachev et al. Sov. Tech. Phys. Lett. 1988, Vol. 14, p. 117
35. I. Abdulhalim, G. Moddel, K. M. Johnson. Appl. Phys. Lett., 1989, Vol. 55, No. 16, p. 1603-1605

## 4. Optically addressed liquid crystal spatial light modulator with the extremely deep phase modulation

### 4.1. Spatial light modulators based on chalcogenide glass photoconductor - liquid crystal structures

The results of the previous section concerning the possibility to realize the deep phase modulation (retardation), using LC SLM can be briefly summarized as follows:

1. There are no physical limitations of the retardation depth. Of, course, the increase of the liquid crystal layer will result in slower performance and, also, in reduce of the modulator resolution. The latter, however, is not too important: assuming the corrector diameter of several centimeters, it is obvious that even the very low resolution of just several pairs of lines per millimeter, would be quite enough for correction for the large scale optics distortions, which usually reveal the rather smooth and steep character, or, vice versa, just abrupt piston shift (non co-phased segmented mirror).

2. The realization of the said deep phase modulation does not meet any significant difficulties while realized in the electrically addressed LC SLM, where the control voltage is supplied by the external source. However, the situation changes when we try to realize the same effect in the optically addressed SLMs. The very simplified explanation of the difficulties looks like following. The most of the elements, which were realized and described in the preceding chapter implement the traditional semiconductors as the photoconductor layers. These media, however, reveal the comparatively small dark resistance. The modulator (photoconductor layer + LC layer) is fed by the voltage. In the dark state, when the resistance of the PC layer is large, nearly overall voltage is to fall only on the PC layer. However, the increase of the LC layer thickness results in increase of its resistance, and, for most of the PC media, the total resistances of both layers will become comparable (it is obvious, that the width of PC layer is limited by the value of several μm and thus the resistance of this layer can not be significantly increased). Real situation requires, of course, deeper explanation, but the idea is clear. The realization of the deep phase modulation in the OA LC SLM requires the application of the PC layers with high

dark resistance. One of such media, which was already tested from that point of view, is the chalcogenide glass.

So, in the scope of the studies, devoted to the evaluation of the possibility to provide the optically addressed phase retardation across the very wide range, we have fabricated the prototype of the modulator, providing such a possibility. The use of chalcogenide glass photo conductive layer with the very high dark resistance made it possible to realize the transparent modulator with the very thick (20 μm) layer of LC and to efficiently use this thickness. Assuming $\Delta n = 0.13$, the physical limit of phase retardation should be ~ 2.6 μm; in fact the measured value was ~ 2.2 μm or 3.5 wavelength of He-Ne laser radiation. The application of the same SLM design in the reflective geometry will provide twice larger retardation. Also, according to our estimations, we have yet the possibility to enlarge the LC layer thickness at least yet twice. So, in fact, the problem of phase retardation across the range of dozen of visible radiation wavelengths can be treated as more or less solved. However, as we shall see, the response time of the element (~ 2 seconds) is rather slow and hardly can be significantly improved.

The transmission SLM (Fig.4.1) consisted of number of thin layers sandwiched between two glass substrata [1]: photoconductor layer, liquid crystal (LC) layer, transparent ITO electrodes, alignment layers. When DC voltage is applied to electrodes, it is divided between photoconductor and liquid crystal layers according to spatial distribution of writing light intensity. Potential relief on the LC layer results in local modulation of optical characteristics of LC layer, such as its optical activity or birefringence. When the reading light passes through the LC layer it is modulated according to the input image distribution. In the transmission mode of SLM realization the reading light passes through all SLM structure layers, including the photoconductor layer. So the reading light must be out of the spectral sensitivity range of the used photoconductive material or to have the intensity in the same spectral range much lower than the writing light intensity [2].

The standard optical glass K-8 ($n = 1.51$; $\rho = 2.52$ g/cm$^3$) was used for preparation of substrata. The glass plates ( diameter - 35 mm, thickness - 6 mm ) had a high optical quality: surface flatness of 1 wavelength per 35 mm at 633 nm (N = 1), local surface flatness $\Delta N = 0.5$.

Transparent electrodes were prepared by cathode sputtering in glow discharge. ITO electrodes that were prepared by this method have high homogeneity of electrical and optical properties. The smallest crystal structure of the ITO layers let us to realize a good uniformity of nematic LC orientation. The ITO electrodes had transmission 80 - 90% in all visible spectral region, conductivity 500 - 1000 $\Omega$/sq., good uniformity optical and electrical characteristics.

The special feature of developed SLM is application of chalcogenide glass semiconductors as material for photo-conductive layers. Use of chalcogenide glass semiconductors (CGS) as photoconductive materials is promising for the optically addressed SLMs. Evaporated layers of this amorphous material have good uniformity of optical and electrical properties. It is possible to modify very easily the spectral sensitivity of PC layers by changing the composition. These materials have low charge carrier mobility, making thus it possible to realize the SLM with the high resolution. For example, in the As-Se system the maximum of spectral sensitivity is changed from 400 to 600 nm when content of As is changed from 5 to 40 % (Fig.4.2). Dark conductivity of thin layers, made of the tested materials was $10^{-12} \div 10^{-14}$ $\Omega^{-1}$cm$^{-1}$. Increasing of As content results in change of the sign of the dominant current carriers. Electrons are dominant current carriers when As content is less than 10 %, and holes when As content is more than 10 % [3].

The dependence of photocurrent J as a function of light intensity N is described by the relation: $J = N^{\alpha}$. Coefficient $\alpha$ was less than 1.0 in the region of N from $10^{12}$ to $5*10^{14}$ quanta/cm$^2$s. $\alpha$ depends on the spectral range and of the sign of applied voltage.

Study of response times of these materials showed that composition $As_{10}Se_{90}$ has the best response times: rise time - 5 ms, decay time - 5 ms.

Study of As-Se system let us to chose the optimal composition for the SLM application. We found that $As_{10}Se_{90}$ is optimal for writing in spectral region 400 - 550 nm, reading at 633 nm and $As_{20}Se_{80}$ - for writing in spectral region 550 - 650 nm reading at 700 - 900 nm.

The photoconductive As-Se layers were deposed by the resistive vacuum evaporation. The vacuum system was supplied by the planetary rotation of substrata

and of the optical interference control of layer thickness. The thickness of used As-Se layers was changed from 0.1 to 1.0 μm.

The important feature of the photoconductive As-Se layers is their very low dark conductivity $10^{-12}$ - $10^{-14}$ $\Omega^{-1}cm^{-1}$, that allows thus to provide the good agreement with thick LC layers. This is important to get the SLM with maximal phase shift, that is defined by thickness of LC layer.

In the SLM we have used the optical birefringence field effect in nematic liquid crystal. Main parameters of the LC-material were the following: $\Delta n = 0.13$, $\Delta \varepsilon = +4.4$, $\Delta t = -20...+90°C$. The thickness of the LC layer was 20 μm. Electro-optical characteristic of the SLM (dependence of the element, mounted between the polarizers, transmission vs. applied AC voltage) is presented in Fig.4.3. Dependence of the phase shift in the element vs. applied voltage (Fig.4.4) was thus reconstructed from the electrooptical characteristics, using the following relationships between the element transparency in crossed polarizers and phase shift (retardation):

$$I = I_0 Sin^2 2\beta Sin^2 \frac{\Delta\varphi}{2} \quad (1),$$

$$\Delta\varphi = \frac{2\pi d\Delta n}{\lambda} \quad (2),$$

here $\Delta\varphi$ - phase shift, d - thickness of LC-layer, $\Delta n$ - optical anisotropy of LC-material, $\lambda$ - wavelength.

The reliable value of the element spatial resolution was 32 pair of lines per millimeter, which is quite enough for the NOF-application. The switching on time, measured for the feeding voltage of 25 V equaled ~ 300 msec, while the switching off time for the same voltage was equal 1.0 sec. The measured sensitivity of the PC layer at 0.63 μm was equal ~ $10x10^{-6}$ $\mu W/cm^2$; for the green radiation this value should be ~ 10 times smaller.

## 4.2. Demonstration of optical addressing of the modulator

The possibility to control the phase retardation in such a wide range ($7\pi$ in the transmissive mode) by means of optical addressing has required the experimental confirmation. So the simplest demonstration experiment was carried out. The modulator was mounted between two crossed polarizers; the angle between their axis

and the director was 45°. Through this beamlet there was going the beam of He-Ne radiation with the diameter of ~ 20 mm. The intensity distribution across the beam section was nearly gaussian. The total power of radiation could have been controlled in the range 0...3 mW. The modulator was fed by the continuous voltage.

Non-uniform spatial distribution of radiation across the section resulted in non-uniform distribution of charges across the photoconductor section. Thus the phase retardation of radiation in LC layer was also non-uniform across the section. So the polarization state of the radiation after the SLM was also non-uniform across the beam section. The use of polarizer - analyzer revealed thus the system of concentric rings in the intensity of one of polarized components (Fig.4.5); the relative phase retardation in the beam section point, corresponding to two neighboring rings, equals $2\pi$ or one radiation wavelength.

For the maximal total power of the He-Ne laser radiation of 3 mW the increase of the voltage, feeding the modulator, resulted in growth of the said rings' number from 0 to ~ 3.5; this growth was saturated when the voltage reached some 40 V. Attenuation of the beam power with the feeding voltage preservation has also resulted in reduce of the rings' number.

So one can see that the described element can be treated as the prototype for the future experiments on NOF-correction with the holographic converter (see Chapters 7 and 8). We can also assume at this moment that the appropriate performance can be realized with the thicker layer of the liquid crystal, of, say, 40 μm.

### References

1. F.L.Vladimirov, A.N.Chaika, I.E.Morichev, N.I.Pletneva, Peculiarities of response time of Spatial Light Modulators based on photoconductor - liquid crystal structures as input devices of holographic correlates, Russian J. of Optical Technology, 7, 1993, 53.
2. F.L.Vladimirov, J.C.Buchholz, High resolution Optically Addressed Spatial Light Modulators using Photoconductor - Liquid Crystal Structures for Real-Time Optical Data Processing Applications, Optics and Information, 6th Topical Meeting of European Optical Society, ESSAIM, Mulhouse, France, 23 - 26 October 1995.
3. F.L.Vladimirov, I.E.Morichev, N.I.Pletneva, T.O.Reshetnikova, Photoelectical characteristics of chalcogenide glass $As_{10}Se_{90}$, Russian J. of Optical Technology, 1985.
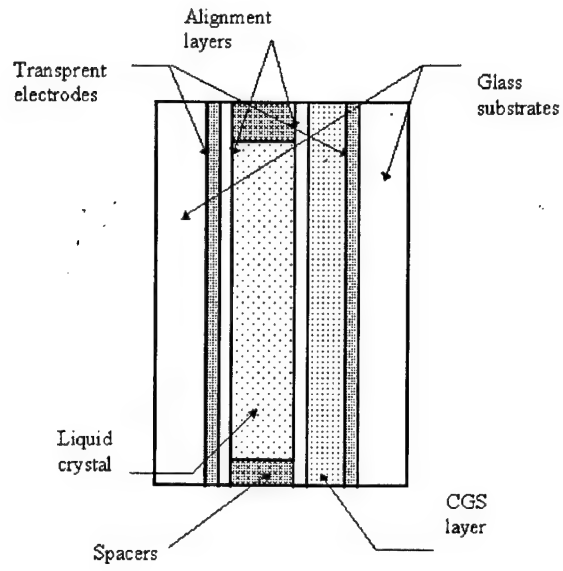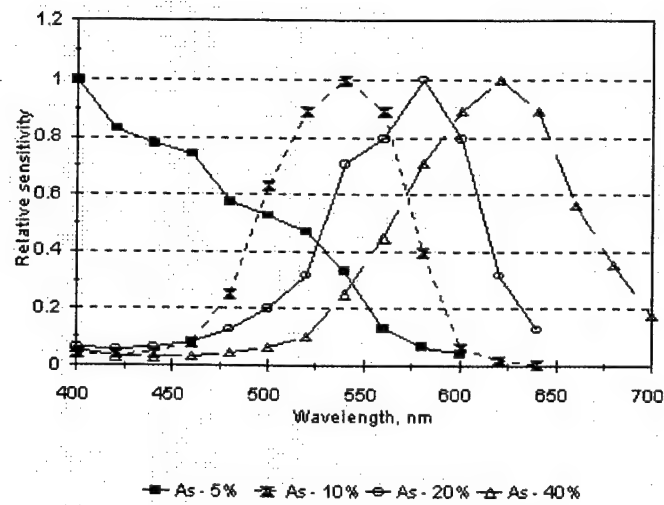
Fig.1. Transparent LC SLM



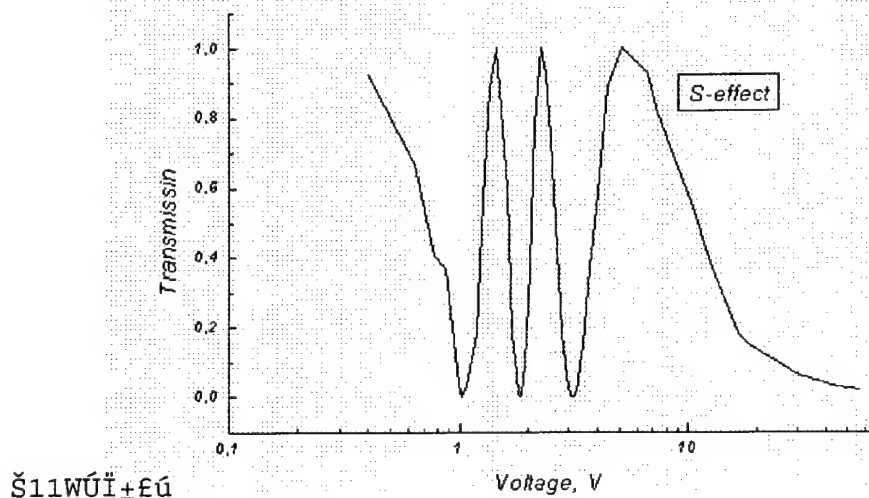Fig. 2. Relative spectral sensitivity of chalcogenide glasses of As-Se system.

Fig. 3. Electro-optical characteristic of the SLM on optical birefringence, thickness of LC layer is 20 μm.
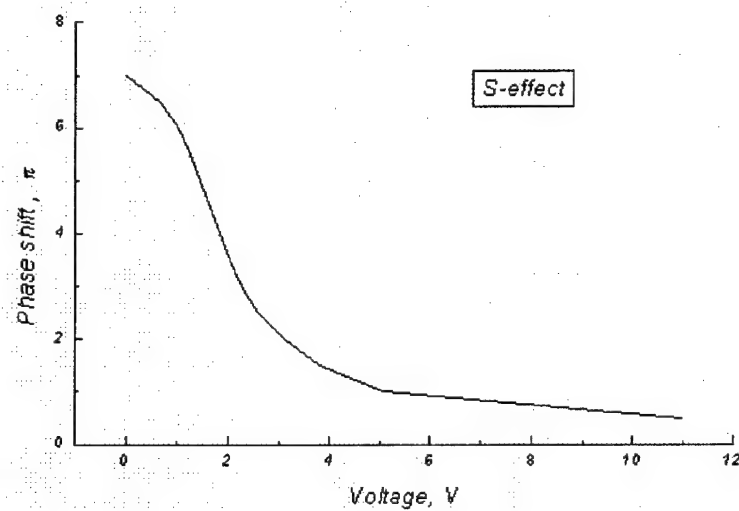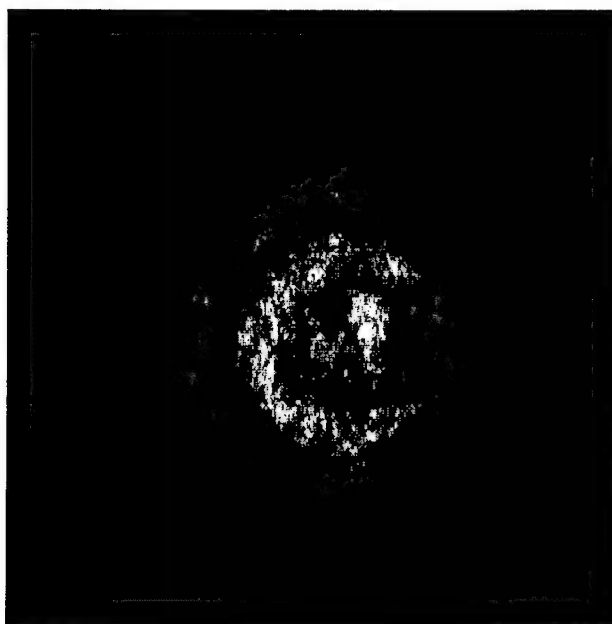


Fig. 4. Phase shift as a function of applied voltage.

Fig.5. Spatial distribution of the gaussian beam after the self-action in the OA LC
SLM, mounted between two polarizers.

## 5. Possibility of EA LC SLM application in NOF-correction schematics

### 5.1. Electrically addressed liquid crystal matrix for adaptive optics

Rather promising approach to the realization of the fast response NOF correction schematics with the deep phase retardation is the use of the electrically addressed matrix of the liquid crystal spatial light modulators (EA LC SLM). Such an element can be controlled by various means, and, in particular, by means of electrical signal, corresponding to some optical pattern, recorded by the auxiliary TV system.

One of the leading positions all around the world in design of the elements of such a class is the private company "Peterlab", St.-Petersburg, Russia. The scientists of this company has kindly provided the results, concerning the latest their elaboration in this field, in particular, the element with the 256 (16 x 16, square shaped) individually addressed deep phase retarders. The size of the overall matrix was 22.4 x 22.4 mm and of the individual element is 1.35 x 1.35 mm; the element spacing is ~ 52 μm; their total number (16 x 16) and square shape provide, in particular, simple conjugation of this device with the standard CCD matrices.

In course of the matrix design there were elaborated the transparent abn reflective matrices, using either the multy-layer dielectric mirror (wide or narrow band), as well as the metallic mosaic mirror. The device is realized on the base of fused silica substrata, subjected to the special laser processing in vacuum, preceding coating by the transparent conductor layer. This processing has removed the cracked layer on the surface and improved the adhesion and damage threshold parameters of the element, which can be, in particular, use for the laser beam profile correction (for the radiation at 1.06 μm, pulse duration 20 ns, the damage threshold exceeded 3 J/cm$^2$).

The very LC corrector is the based on LC cell with the diameter of 50 mm. In the Fig.5.1 in the scale 1:1 is shown the contact part of the element, using four standard 64-contact connections and the anisothropic conducting rubber.

The transparent LC cell was tested while filled by two types of the nematic LC with the high value of $\Delta n$ ~ 0.2 and different viscosity, which determines the response time. The phase retardation of the element vs. applied voltage was measured as in the S-cell, mounted under the angle of 45 degrees between the crossed polarizers; radiation wavelength 0.63 μm (He-Ne laser).
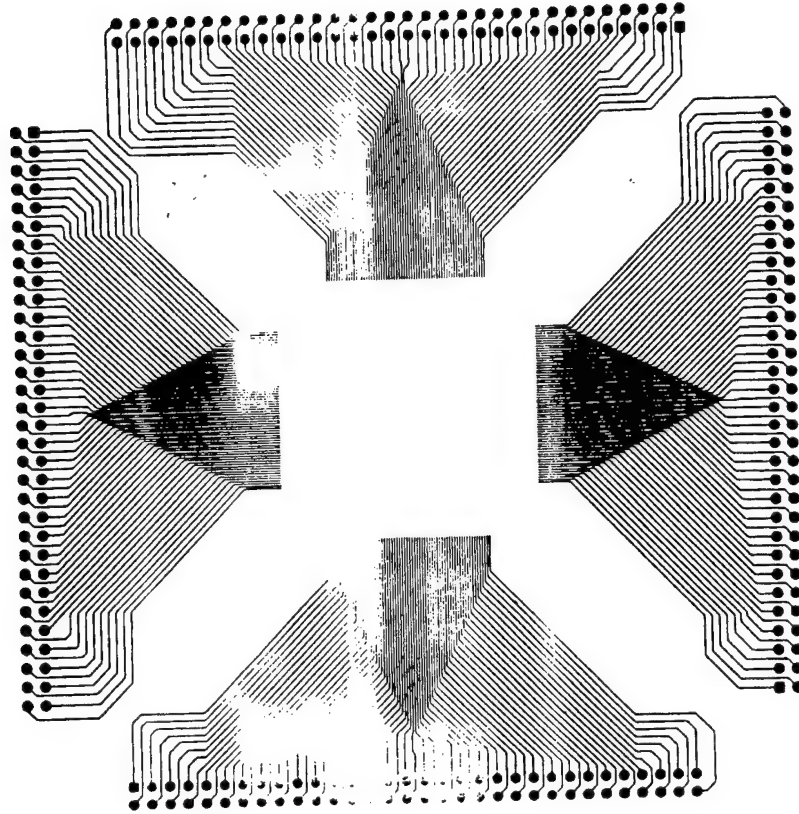
Fig.5.1. Contact part of the cell (natural size)

The transparency of the cell is varied with the phase shift as $I \sim I_0 \cos^2 \frac{\delta}{2}$, where $\delta = \frac{2\pi d}{\lambda} \cdot \Delta n$; for the cell with the LC layer of 10 μm thickness the maximal phase retardation has to be about $6\pi$. This value was experimentally confirmed; the feeding voltage was varied from 0 to 40 V. So in the matrix there was realized the small angle of hanging of LC molecules. The reflective cell with the same thickness of LC layer would provide phase retardation of $12\pi$, and, according to our estimations, in the nearest future we shall realize the element of double thickness, providing the overall shift of 24μm or, in other terms of ~ 15 μm, which would be quite enought for the application discussed in this Report.

Temporal behavior of the device was measured for two types of the nematic LC and for two kinds of the orientants: the oxides with the tilted deposition and the rubbing over the polymer. To this moment we have realized the following set of parameters; to our opinion, their values are determined first of all by the feeding scheme and not by the very LC properties.

The device was fed by the rectangular pulse with the duration of 10 ms and voltage of 10 V. The switching on time was < 100 μsec, while the switching off time equaled ~ 50 msec for the layer thickness of 5 μm and ~ 100 msec for 10 μm. So the element of such design provides operation with the characteristic frequency of ~ 10 Hz; the elaboration of the orientants promises its improvement in at least several times.

## 5.2. TV controlling system

In the case of the above described application for the NOF-correction one has to control the retardation matrix by the analogous means of intensity distribution across some optical pattern, i.e. by the TV signal. Of course, there are possible a lot of variants of the system realization. However, most of them would require elaboration of special electronic hardware, which can be done only for the real system design. With respect to the method feasibility demonstration experiment (see Chapters 7 and 8) one can speculate concerning three variants of the TV control contour realization.

In the Fig.5.2 is shown the control by means of the TV matrix (camera), consisting of the discrete elements. The signal from the output of each element is amplified in the amplification unit and is sent for the optical modulator control.

In the Fig.5.3 is shown the second variant of the control, in which the image is recorded by the TV camera, using the CCD matrix. This matrix is connected with the personal computer via the interface. The corresponding software provides import and processing of the image and the output of the controlling signals (for example, via the parallel port). The controlling signal is distributed across the elements of the modulator matrix is realized by the demultiplexor.

The third variant of control hardware is shown in the Fig.5.4. In this case the image is recorded by the CCD-matrix. Special control unit controls this matrix and provides image processing. The same device provides the signal for the modulator control, which reach it also via the demultiplexor.

The realization of the 1st variant will need special design and fabrication of the discrete photosensor matrix and of the amplification unit; that of the 2nd variant - of the demultiplexor and of the software; other elements are market available; and that of the 3rd variant - of the CCD-camera control unit and of the demultiplexor. The 1st and 3rd variants would be rather rigid and would not provide the possibility of fast and cheap modification in the conditions of the experiment.

47

So, seemingly, the proposed demonstration experiment (see Chapters 7 and 8) is to be based on the variant 2. Market available are, for example, the CCD camera Electrim EDC-1000D with the interface for the IBM PC compatible computer; our estimations show that such a design will provide the output control signal modification with the frequency of at least 2 Hz, which is enough for the demonstration experiment.
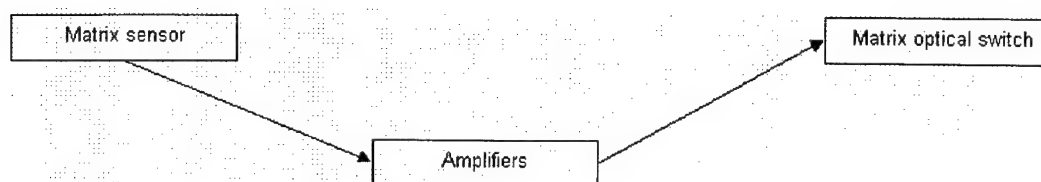


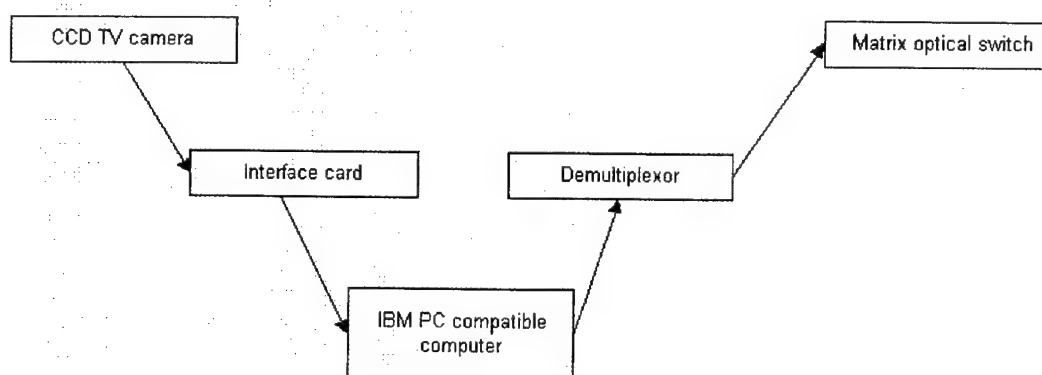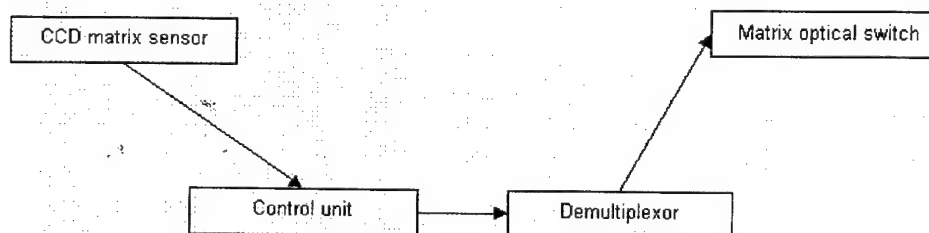Fig.5.2. Direct connection of matrix photosensor and modulator



Fig.5.3.



Fig.5.4.

## 6. *Optimization of optical schematics of NOF-correction with the use of holographic converter*

The basic goal of this study is the elaboration of the scheme of possible experiments on feasibility of the NOF-correction schematics, providing correction for distortions with the large magnitude in the wide spectral range. Hence it is reasonable to discuss several specific problems, such as the choice of optimal scheme of holographic interferometer with the expanded range of monotonous variation of the output signal intensity, on the correction ability of the system and on possible approaches to the feedback loop locking.

### 6.1. Optimal scheme of holographic interferometer

Special feature of NOF-correction schematics is the necessity to organize the propagation of distorted optical waves, bearing the information on the distortions of optical elements to be corrected for. In the case of the novel approach to NOF-correction, discussed in this Report, the magnitude of these distortions would be rather high. At the same time the complicated character of this schematics results in the necessity to implement the sufficiently long optical relays. On the long optical path the phase distortions of the wavefront can transfer to the amplitude one, resulting hence in deterioration of correction ability and so in the system performance aggravation. In particular, the primary schematics of NOF-correction with the holographic converter of distortions scale (see Interim Report #1), shown in the Fig.6.1 , there are several such paths with the sufficient length. In the Figure the shadowed zones correspond to the ranges of propagation of significantly distorted beams. The situation would be yet more complicated in the scheme with the purely optical relay of interference pattern in NOF-loop.

With this respect the following requirement to system schematics is to be fulfilled. The length $L$ of optical beamlets is to be significantly smaller than the characteristic length of diffraction mixing of the beam $l = d/\lambda^2$, where $d$ is the characteristic transverse size of wavefront distortion. The radical solution is to use the auxiliary lens relays, re-imaging field distributions along the system. This approach, however, results in significant further complication of optical schematics and in extra sources of distortions and optical noise. At the same time, the schematics, shown in the

Fig.6.1, is already rather complicated and it should be reasonable to find out the simpler schematics, implementing the proposed principle.

Such a schematics was elaborated during the second stage of the work; it is shown in the Fig.6.2. In this variant of NOF-correction scheme with the holographic converter the significantly distorted waves on both wavelengths propagate along one and the same and the only comparatively short beamlet. Then one of them is used for dynamic hologram registration and the second one for its reconstruction, resulting in reconstruction of the wave with the differential, i.e. significantly reduced in their magnitude, wavefront distortions, which is then used in NOF-correction. One can see also that this variant of the system is simpler and contains lower number of principle elements than the one shown in Fig.6.1.
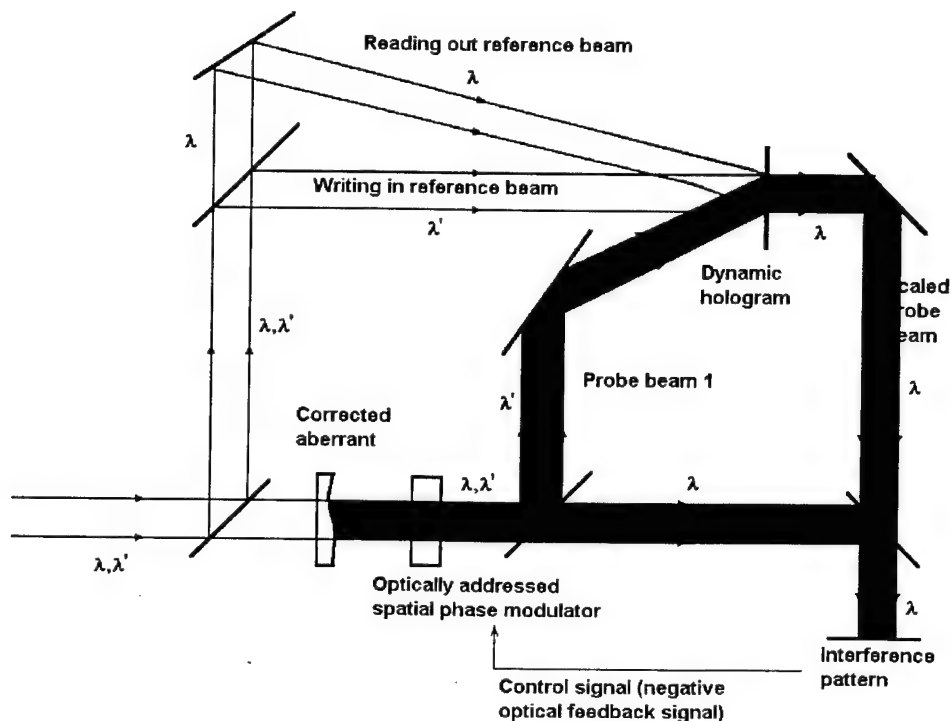


Fig.6.1. Propagation of robustly distorted wavefronts in the scheme with interference of the beams with the scaled and non-scaled distortions.
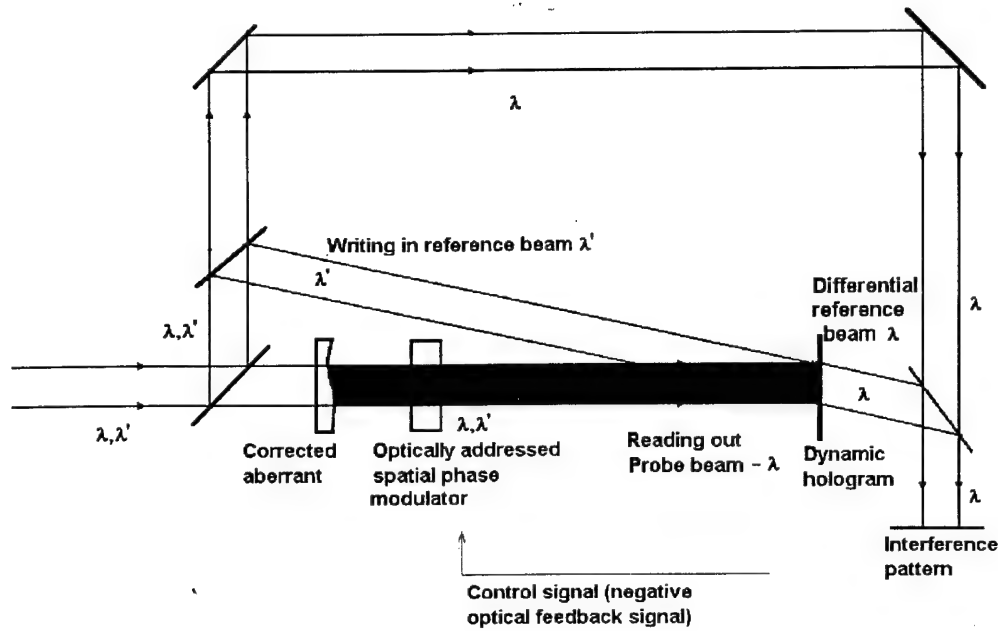
50

Fig.6.2. The scheme with the reduced length of robustly distorted wavefront propagation.

## 6.2. NOF schematics: correction opportunities.

It is fairly obvious that the NOF scheme using the holographic converter, from the point of view of correction opportunities, does not differ essentially from its prototype - ordinary NOF system. One should only to replace the real wavelength of auxiliary optical radiation $\lambda$ to the effective value $\Lambda$ (see Chapter 1). At the same time, the essential extension (probably, in tens times) of corrected distortions range prompts us to pay more attention to such characteristics as the value of residual wave front distortions, the influence of the temporary instability and spatial heterogeneity of auxiliary laser radiation, and the time-dependent dynamics system onto its operational mode. With this purpose, within the frame of the present work, the cycle of calculations was done simulating system operation, in the elementary mathematical model of the system. Basing on the remarks mentioned above, all essential effects can be analyzed for the basic NOF scheme; one would substitute when necessary the effective value of wavelength $\lambda$.

Let us consider a point correction problem. Assume that the driving optical field is formed by the interference of two light waves of equal intensity $I_{1,2} = 1$. One of these waves is plain while the another wave front is deformed by joint action of time-

constant aberrator, and time-dependent phase modulator. Let the action of this element is equal to zero when the intensities of those two beams are added (i.e. at mutual shift of phase is $\lambda/4$, that corresponds to summary beams intensity equal 2), and this action is linear to the driving field intensity. That means that the optical delay is expressed as $\delta I = K (I_1+I_2-2)\lambda$. Let assume also that that our system is adjusted optimally, i.e. at the absence of distortions which are brought by the aberrator, the value $\delta I=0$. In such system the distortions of wave front in the range from $-0.5\lambda$ ($\Lambda$)to $+0.5\lambda$ ($\Lambda$) can be corrected

The calculation of current meaning of the optical delay was made by an iterative method. The time delay of the subsequent iteration to the previous relied equal to 1/100 of the phase modulator response time. The response time is defined as the time of transition of the modulator from initial to final state after the step change of driving optical signal intensity of a managing optical signal. For the iteration process, such discreteness allows to represent the exponent by linear sections. After 50-200 iterations the system came in the stationary condition. The significant time lag was observed at the edges of corrected distortions range, at the values close to $-0.5\lambda$ ($\Lambda$) to $+0.5\lambda$ ($\Lambda$). Accordingly, the ranges for modeling were chosen a bit more narrow, about $-0.4\lambda$ ($\Lambda$) to $+0.4\lambda$ ($\Lambda$).



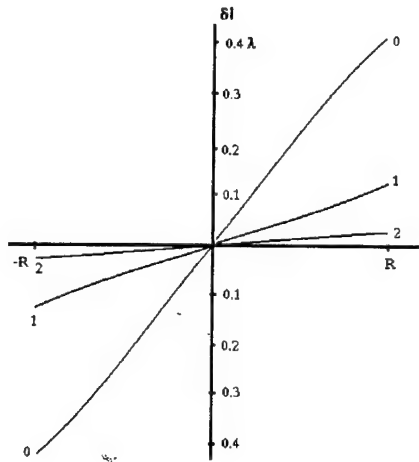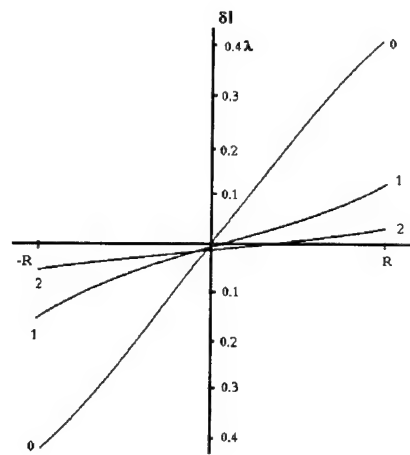Fig.6.3. Correction for wedge distortions. Intensity I=1, curve 0 – noncorredted wedge, 1 – corrected with K=1, 2 – K=4

Fig.6.4. Correction for wedge distortions. Intensity I=0.9, curve 0 – noncorredted wedge, 1 – corrected with K=1, 2 – K=4

The dependence of residual distortions of wave front in the stationary condition is shown in Fig.6.3 for two values of parameter K=1 and K=4 (curves 1 and 2); the initial wedge distortion brought by the aberrator is shown as curve 0. For large K the curves practically coincide with the abscissa axis (see below). One can see that for K = 1, the distortions are corrected approximately to 3 times, and this probably is not enough for many applications. At the same time, for K=4 the residual distortions are reduced approximately in 20 times as compared with initial. This approximately corresponds to the value of residual wave front distortions in high aperture non-reciprocal telescopes [6.1] and can be considered as sufficient.

The essential is the problem of influence of the auxiliary laser radiation fluctuations in spatial and time domains on the correction efficiency. The results of the corresponding modeling are shown in Fig.6.4. Let us assume that, under the same conditions as in a case of Fig.6.3, the intensity of both laser beams has decreased to $I_{1,2}$ = 0.9. In this case the equilibrium point in he aberrator absence is displaced, and the curves of residual distortions are slightly deformed. At the same time, from the data of Fig.6.4 it is visible, that at a rather soft limit in 10% on time stability and of intensity spatial uniformity, such deformation is insignificant.
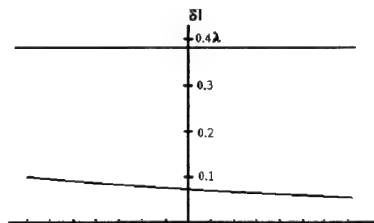


Fig.6.5. Correction for phase retardation (upper curve – noncorrected); parameter K varies from 1.5 (left) to 3 (right side).
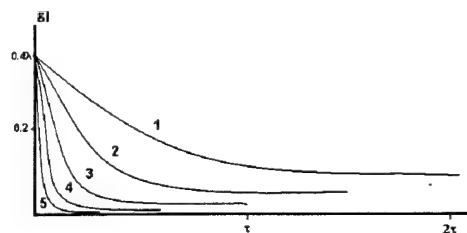
Fig.6.6. Temporal dependence of output phase retardation for various K: curve (1) – 1, (2) – 2, (3) – 4, (4) – 8, (5) – 16

One of essential advantages of NOF system using OA LS SLMs as compared with linear adaptive optics systems using the same wave front actuator [6.2], is the reduction of requirements to optical quality, uniformity and reproducibility of actuator parameters. In our case this element is included itself inside the loop of distortions correction. The opportunity of correction for distortions that are caused by modulator

substrates, wedge distortions in LC layers, etc, is obvious from the very optical scheme (see Fig.1.1). At the same time, the reduced sensitivity of system to the time reproducibility and spatial uniformity of the modulator parameters is visible from results of modeling, Fig.6.5. Distortions in the range of $0.4\lambda$ were corrected by the modulator with parameter K varying in cross section from 1.5 up to 3.

The time behavior of residual error is shown in Fig.6.6: in parallel with growth of the feedback parameter K the turn-in time is reduced.

## 6.3. Optical feedback loop locking

The specific feature of the scheme proposed is the unusually deep phase modulation in OA SLMs. This feature affects not only the problem of an adequate OA SLM design (see Sec.3) but also a question of the circuitry of an optical system locking the optical feedback loop, i.e. a system carrying the signal intensity distribution from the interferometer output to the SLM photoconductor layer.

Such locking system can be arranged either using purely optical means, with beamsplitters, mirrors and optical relay systems (Fig.6.7), or by optoelectronic means (Fig.6.8 - with auxiliary optical projecting system, or Fig.6.9 - with contact transfer of the optical image from TB-tube on a photoconductor directly or by fibers bundle).

The advantages of the first approach: simplicity and cheapness of optical components, and the absence of additional delays connected to transformation of a signal in TV-systems. At the same time this approach has a number of lacks, among them:

• The penetration is practically inevitable of a part of the reading optical signal from the probe interferometer branch to the photoconductor layer; this results in parasitic noises, including speckle noise;

• It is necessary to maintain the certain level of intensity on a photoconductor; this requirement, because of light losses in holographic corrector, results in unnecessary high signal level inside interferometer;

• The requirements to adjustment accuracy and stability are much more rigid then in the schemes using TV-devices;

• The spectral limitations occur connected to selection of lasers and sensitivity of photolayers.

54

The schematics using TV-devices has no such lacks; besides it has essential advantages. First, one can increase the depth of phase modulation using a sequence of modulators driving by the same optical signal; this can be easily done using TV-devices (Fig. 6.10).

Another problem to be discussed is that of the systems with increased feedback coefficient K. As it is clear from results of the previous paragraph, at K = 1, that corresponds to phase shift within the limits of one wave length (real or effective) at change of driving intensity from a minimum up to a maximum, the degree of correction is not high enough. One of the possible solutions of the problem was marked in the Interim Report #1: this is two-step circuit of NOF-correction including the step of rough correction with the holographic converter, and the step of fine correction using the traditional approach; such circuit, however, is rather bulky.

Another possible solution is the direct realization of system with increased feedback coefficient K: the whole change of driving light intensity corresponds to phase shift in wavelengths (real or effective). This approach is hardly rational, as it requires a further increase of thickness of the modulating layer, at preservation of corrected distortions scale.

The question on an opportunity to solve the problem by pure optical means is not clear yet, and requires additional studies. At the same time, in the case of optical feedback loop locking using TV-devices one can speculate on the opportunity to solve the problem by the use of radio engineering or logic methods: one could use in TV-loop a circuit with a certain nonlinearity of the output intensity from the input.
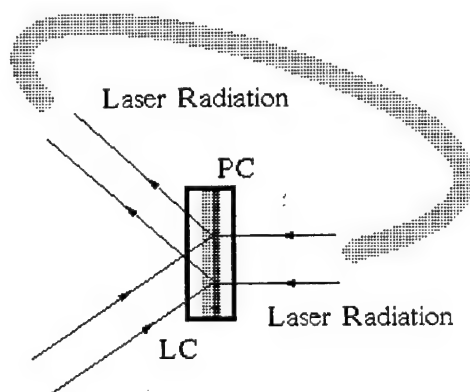
Fig.6.7. Direct control of SLM by the very laser radiation. Advantage: simplicity. Disadvantages: noise due to light penetration; difficulties in tuning control radiation intensity
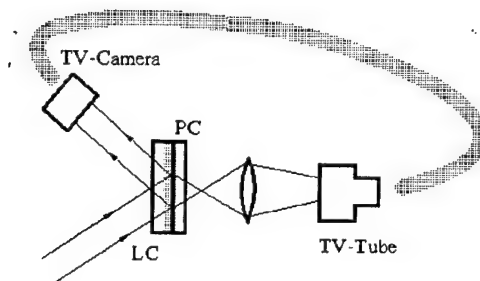


Fig.6.8. Feedback lock by the system: TV-camera-TV-tube-projectile optics-OA SLM
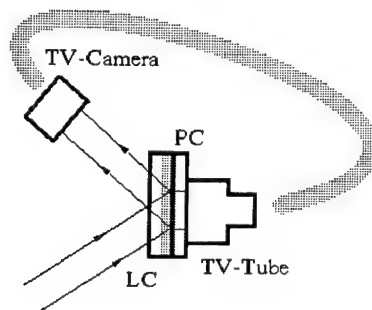


Fig.6.9. Use of pair TV-camera - TV-tube, united with SLM for feedback lock (optically addressed or direct electronic control). Advantages: no penetration noise; possibility of electronic amplification and tuning of signal; conjugation of pulsed mode of dynamic hologram record and CW NOF behavior; easier multiplication of LC layers:



Fig.6.10. Multiplying of control signal by TV locking use.

## 7. Possible scheme of the feasibility demonstration experiment

On the base of the discussion, presented in Chapters from 1 to 6 we can now outline the possible schematics of the experimental activity, aimed onto the demonstration of the proposed method feasibility. It is supposed to be done in course of our future activities (see Chapter 8). The goal of the experiment is:

- to demonstrate the NOF-correction for the model wavefront distortions with the magnitude of at least 3-4 wavelength of visible radiation;

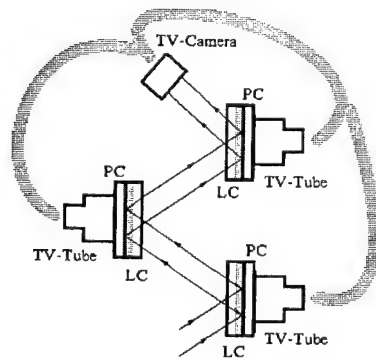- to evaluate several variants of corrector, based on deep phase retardation in LC SLM, in particular, the scheme, based on the OA LC SLM with the high dark resistance photoconductor and the scheme based on the use of the EA LC SLM, controlled by the optical pattern, registered by the auxiliary TV-system;

- to evaluate the system response time and the residual distortions.

The experimental investigation will result in elaboration of the optimal corrector schematic, which can be used for the correction of the real optical system distortions in wide spectral band.

The possible optical scheme of the variant of the experiment, based on the use of the OA LC SLM, is shown in the Fig.7.1. The dual wavelength ($\lambda_1$ and $\lambda_2$) radiation is provided by two laser sources. In the figure the green and red lines correspond to the beams of this and that wavelength (the colors are arbitrary); the brown lines indicate the joint propagation of the radiation at both wavelengths.

Concerning the choice of pair of lasers. In fact, the most simple variant is to use one and the same laser source for generation of two wavelength of radiation: one can use Ar-ion laser, say its emission at the most intense lines of 514 and 488 nm. In this case we shall automatically provide the mutual adjustment of two beams and shall need to use smaller number of mirrors and auxiliary elements. However, the differential wavelength of $\sim 1/20\lambda$ can be too small for the successful experiment; the possibility of the holographic converter to operate with such a differential wavefront distortions is to be evaluated in course of the proposed experiment. So in the figure there is shown the more complicated, reserve variant of the scheme, based on the use of two separate laser sources L1 and L2: one of them, most probably, would be the He-Ne laser, while

another - the same Ar-ion laser or CW Nd laser (second harmonics); in this case there will be realized the differential wavelength of $\sim 1/6\lambda$, which can be more convenient.

The radiation from both laser sources passes through the auxiliary optical elements and the system for the optical beams parallelism. The focused beams of both lasers create the reference point source of radiation A. This point is optically conjugated with the point X, where can be placed the imaged object, illuminated by or emitting the wide spectral band incoherent radiation. The mirror C sends both laser beams to the very system of NOF-correction, rounded by the dotted line. It is supposed that nearby the mirror C there will be introduced wavefront distortions to be corrected for. The simplest variant of distorter can be just the used of two segment mirror with the mutual piston shift and tilt.

The correction systems work as follows. The distorted beam, reflected by the mirror C, enters the corrector unit. The pair of lenses 1 and 2 (with the intermediate small-size plain mirror 6) forms the parallel beam. Semi-transparent mirror 3 sends some part of laser radiation into the very corrector - the liquid crystal layer of the reflective (mirror) "thick" LC SLM M1; the variants of this element to be used in the supposed experiment are discussed further in this chapter. Residual part of radiation from the laser and thermal sources source passes through the mirror 3 and enters the recording system 4, used for the control of the distorted image.

The mirror-like corrector is mounted nearly orthogonal to the incident beam. Some part of the radiation, reflected by the corrector mirror passes through the mirror 3 and enters the second recording system 5, used for observation of the corrected image of laser and thermal objects. Another part of the reflected radiation passes through the gap between the mirrors 6 and 11 and is collected by the lens 7. Mirror 8 sends it to the OA LC SLM M2, used for the dynamic hologram-converter recording.

Part of radiation from laser source L1 at the system input is split off by the semi-transparent mirror 9. The lens 10 focuses it to the focal plane of the lens 7, forming thus the plain beam at the wavelength $\lambda_1$. This beam interferes with the probe beam at the same wavelength and thus the transparent dynamic hologram is recorded in the SLM M2. The radiation at the wavelength $\lambda_1$ passes through the dychroic plain mirror 12 and leaves the systems. The probe beam of the radiation at the wavelength $\lambda_2$ is used for the said dynamic hologram-converter reconstruction. The reconstructed

beam with the differential distortions of the wavefront (see Chapters 1 and 6) is reflected by the said mirror 12 and enters the feedback loop scheme. The lenses 13 and 14 form the 1:1 telescope, used for spatial filtration of the residual zero-order diffraction beam at the wavelength $\lambda_2$ (screen S) and, if necessary, the small-scale noise (arbitrary pinhole, not shown in the Figure). The mirror 15 sends this differential probe beam of radiation to the photoconductor layer of the OA LC SLM M1.

The semi-transparent mirror 16 splits off some part of radiation at the wavelength $\lambda_2$ from the laser source L2 to the beam expander 17. The expanded beam with the plain wavefront passes through the semi-transparent mirror 15 and forms the reference beam for corrector controlling. The radiation, reflected by the backward side of the corrector element is then blocked by the screen S. The optical delay between the elements 16 and 17 can be used also for proper tuning of the relative phase shift between the probe and reference beams, used for the corrector control.

The given geometry of the system provides the possibility to organize the image relay (retranslation) through the system. The lenses 1 and 2 work as the achromatic pair, imaging the distorting mirror C to the plain of modulator-corrector M1. So the wavefront distortions are relayed to this plane, where the average shape of the wavefront would be plain.

The achromatic aberration-less pair of lenses 2 and 7 relays the radiation from the plane of the element M1 to the plane of the hologram-converter M2. Then this plane, in turn, is relayed by the aberration-less (but not necessarily achromatic) pair of the lenses 13 and 14 to the plane of the photoconductor layer of the modulator-corrector M1. Note also, that these relays provide the possibility to provide the proper overlap of probe beam and control radiation beam in the element M1 without any auxiliary image rotating elements, like Dove prism, which were widely used in previous experiments.

Concerning the corrector element itself. It is supposed that in the course of experimental work we shall try at least two types of the LC SLM, providing deep dynamic retardation of the beam - the optically addressed LC SLM and the electrically addressed, controlled by the optical pattern.

**1. OA LC SLM.** In the Chapter 4 we have discussed the prospective approach to the "thick" OA LC SLM realization, based on the application of the high dark resistance photoconductor layer, made of the chalcogenide glass. It was shown that such a modulator can provide deep phase retardation of the beam. So it is planned to realize the reflective (mirror) variant of the modulator and to use it in our experiments. The mirror-like SLM provides, first, the doubled depth of phase modulation, and, second in most cases of NOF schematics it provides the simpler geometry of the scheme. Moreover, in the case of chalcogenide PC layer the use of reflective geometry is practically inevitable. The reason is that the said compound absorbs the radiation in the overall visible range of spectrum. Hence, the application of transparent geometry (see Chapter 6) is possible only for the signal correction in the IR range of spectrum.

However, the mirror-like geometry imposes some novel technological problems. As it was already discussed in Chapter 3 and references there, one can use either solid dielectric mirrors in the LC SLMs or the multy-facet metallic mirror. Obviously, from the point of view of electric scheme the use of the solid dielectric mirror is possible only in the SLM, fed by the pulsed voltage. However, the advantage of the very high resistance of the chalcogenide PC at the same time obviously prevents its application in the SLM, fed by the pulsed voltage.

So the only way to realize the mirror-like SLM is to use the multy-face metallic layer on the boundary between the PC and LC layers. Such a multy-facet mirror, which is often used in the standard EA LC SLM elements looks like the pattern of metallic polygons (squares or hexagons), separated by the transparent gaps, non covered by the metal. This structure is usually deposed onto the PC layer surface; the usual size of this "mosaic" element is several dozen - several hundred μm; the gaps between these elements has the smaller but the comparable width. This moment is usually treated first of all from the point of view of the element resolution (the resolved element can not be smaller than the size of this mosaic element). However, in our case, as we have said already, there are no specific requirements to the resolution of the "thick" SLM. Nevertheless, in our case the problems in NOF-schematics realization can be caused by the too wide transparent gaps between the mosaic elements.

The application of the OA LC SLM in the geometry of the Fig.7.1 means that intensity of radiation in the interferometer branch of the system is at least not less (and,
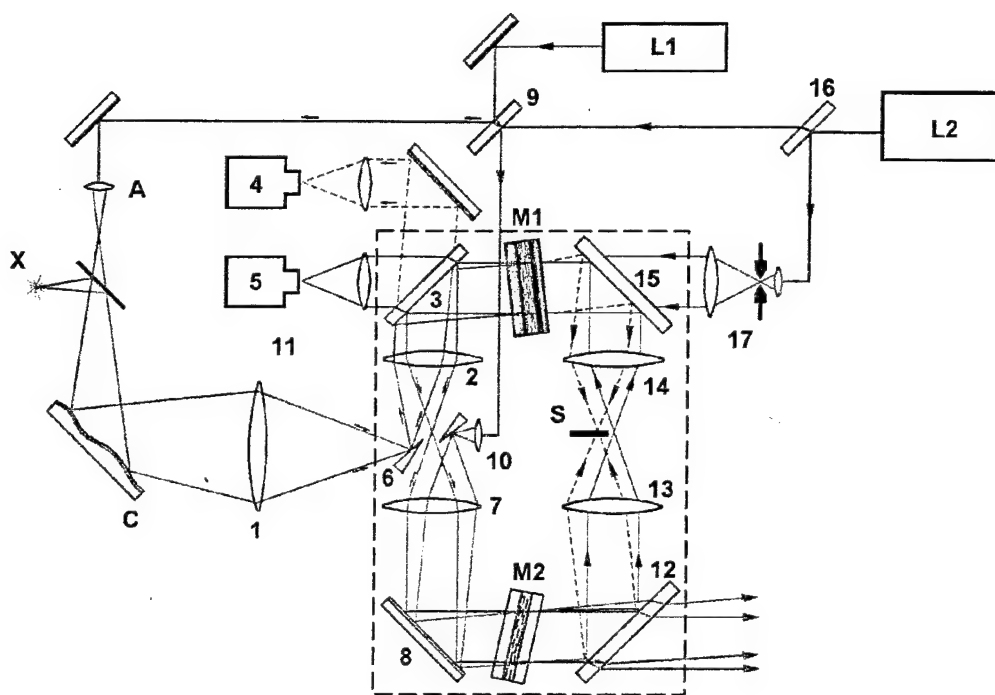
Fig.7.1. Possible optical schematics of demonstration experiment on NOF-correction
with holographic converter feasibility

in fact, much higher due to the energy losses while radiation relay and, especially, due to the diffraction on the dynamic hologram) than in the branch of NOF-loop. In the case when the width of the transparent gaps in mosaic mirror is comparable with its elements size the significant part of the radiation from the interferometer branch will penetrate to the PC layer from its "backward" side and thus result in significant noise. The coherent nature of radiation means that this noise would be the speckle nature, increasing significantly its modulation and thus danger of the improper performance of the scheme.

There are possible two variants of this problem solution:

1) To fabricate the mosaics with the significantly reduced ratio of the gap width to the element size. It requires some elaboration of mosaic deposition technology, which is supposed to be done in course of our future activities (see Chapter 8). It can be done by means of: (a) some increase of the mosaic element size (we yet do have some reserve for reduce of the element resolution - the element described in Chapter 4 has revealed the resolution of ~ 15 mm$^{-1}$- which can be reduced yet several times) and (b) modification of mirror deposition technology, resulting in narrower gaps.

2) To fabricate the element, using the auxiliary non-transparent, light blocking layer. This technology, to the best of our knowledge, was not yet realized in practice; we suppose to do it in course of our future activities (see Chapter 8).

**2. EA LC SLM, combined with the TV contour.** In the Chapter 5 we have discussed the possibility to implement in the NOF-correction schematics the matrix electrically addressed LC SLM, controlled by the optical pattern, transformed in the TV contour.

It is planned that on completion of the experiments with the OA LC SLM the setup, shown in the Fig.7.1, will be modified so as to evaluate the possibility of such a combination use. In this case the overall schematics is preserved, but the final image of the distorter is to be relayed not to the backward side of the SLM, but to the TV camera. All other relays and clean-ups of the beam are to be preserved.

The schematics of the electronic unit to be used is the one described in Chapter 5.2. It is supposed that to the moment of the supposed experiment there will be available the matrix element of EA LC SLM with the dimension of 16 x 16 elements. Obviously, it is not a very large number. The action of this element is similar to the set

of 16 x 16 plain phase retards, piston shifted one with respect to another. In fact, the proper correction for the smooth distortions requires that the wavefront deviation gradient is approximated by piston shifted planes with the sufficiently small separation. The diffraction limited performance requires that such plain segments are separated by the shifts of not more than $\lambda/8$. So in our case of 16 elements across the corrector the maximal possible deviation of the wavefront from some ideal surface would be not more than $2\lambda$. However, the positive effect of the correction can be observed also for the distortions with the larger magnitude. This item is to be the subject of the theoretical and experimental study, described in Chapter 8.

## 8. Feasibility study of the dynamic correction for robust wavefront distortions, using LC SLM corrector in the sophisticated NOF schematics (work proposal)

### 1. Introduction and background

Recently proposed novel sophisticated schematics of the analogous, computation-free, cheap technique of nonlinear-optical correction for distortions, using the liquid crystal spatial light modulator (LC SLM) in the negative optical feedback (NOF) loop, promises the correction for the large scale wavefront distortions, imposed into the wide spectral band optical beam (image) by the large scale optics and distant optical beamlet defects and distortions. This novel schematics is based on the implementation of the sophisticated interferometer schematics, using the holographic converter for the wavefront distortions' scale, based also on the LC SLM application. Such an interferometer provides the output dual wave interference pattern with the significantly extended period of output intensity modulation vs. relative phase retardation of two beams.

The preceding theoretical analysis and the preliminary technology studies has confirmed the possibility to carry out the demonstration experiment of the method feasibility. Available now are the key elements of the system, namely the "thick" LC SLMs, providing the real time extremely deep optically addressed phase retardation modulation, as well as the recording of the sufficiently efficient thin dynamic holograms with the possibility of reading out by the radiation with the significantly shifted wavelength with respect to that used while this dynamic hologram recording. However, some additional technology studies are yet necessary.

In course of the preceding activities there was elaborated the improved schematics of the experiment, based on direct reconstruction by the said holographic converter of the wavefront with the distortions of the differential (significantly reduced) scale with respect to those imposed by the distorting elements and beamlet. Numerical simulation has shown that even in the simplest schematics of NOF it is possible to reduce the wavefront distortions at least 3-4 times.

## 2. Work goal

The goal of the work is the experimental and theoretical study of the possibility to implement the LC SLM in NOF loop as the nonlinear-optical corrector for distortions in the wide spectral band, including:

- fabrication of the optically addressed (OA) LC SLM, providing deep phase retardation;
- fabrication of the electrically addressed (EA) matrix LC SLM, providing deep phase modulation and controlled by the optical pattern;
- fabrication of the thin dynamic holographic converter, based on the use of OA LC SLM;
- experimental demonstration of the correction for distortions in real time with the use of elaborated LC modulators;
- clarifying of the requirements to the elements of the large scale optical observational telescopes.

## 3. Technical parameters of the experiments

The feasibility experiment is to demonstrate the correction for the huge (at least 4-5 visible radiation wavelength) distortions, imposed by the model distorters in the overall visible spectrum to the image, recorded with the use of thermal radiation source.

The experiment is to be based on the use of auxiliary dual wavelength source of coherent radiation (two lines of Ar-ion laser emission). The holographic converter will be based on the optically addressed LC (nematic or ferroelectric) SLM. Two variants of the deep phase retardation NOF-correctors are planned to be probed:

1. OA LC SLM corrector, based on the use of the photoconductor layer with the very high dark resistance, using the chalcogenide glass technique.
2. Matrix EA LC SLM corrector, controlled by special TV system, registering the optical control pattern.

| | |
|---|---|
| Spectral range of correction | visible light |
| Response time | 0.5...15 Hz |

| | |
|---|---|
| Corrector diameter | ~ 30 mm |
| Phase retardation depth | > 3 μm |
| Imaged object | thermal objects |
| Performance | nearly diffraction limited |

## 4. Content of the work

It is planned to carry out the following investigations:

1. Experimental investigation (demonstration experiment) of the imaging of the thermal object with the NOF-correction schematics with the dynamic holographic converter, using the dynamic corrector, based on the "thick" OA LC SLM and on the "thick" EA LC SLM, controlled by the TV-contour.

2. Technological elaboration of the "thick" OA LC SLM, based on the application of the photoconductor layer with the high dark resistance (chalcogenide glass); mastering of the element fabrication technology; fabrication and optical testing of the elements, including the elements with the modified mosaic mirror and with the blocking optical layer.

3. Elaboration of the technology of the matrix EA LC SLM, controlled by the optical pattern, recorded by the TV-contour. Experimental testing of the apparatus.

4. Theoretical and numerical study of the system performance and correction ability, accounting for the special features of the elements used. Elaboration of optical schematics and technical requirements for the corrector unit to be used in the experiments on the distortions correction in real imaging telescope, working in the wide spectral range.

The work is to be carried out on the base of existing theoretical and experimental base and is to be finished by experimental demonstration of the unit for dynamic correction for distortions.

## 5. Work schedule and expenditures

### A. Expenditures:

| | Cost (US $) |
|---|---|
| **1. Purchase** | |
| Ar-ion laser | 10,000 |
| OA LC SLM for holographic converter | 5,000 |
| "Thick" OA LC SLM for NOF-corrector (3 items) | 10,000 |
| (2 elements with modified mosaics, 20 and 40 μm layers | |
| of LC; 1 element with light blocking, 20 μm layer of LC) | |
| Matrix "thick" EA LC SLM | 10,000 |
| TV system for the matrix element control | 10,000 |
| Optical elements (achromatic lenses, dychroic | 5,000 |
| mirrors etc.) | |
| **2. Labor cost** | 25,000 |
| **3. Overhead expenditures** | 15,000 |
| **Total:** | **80,000** |

### B. Tentative work plan

1. Fabrication and testing of the thick optically addressed LC SLM.

Tentative cost - 15,000 $

2. Design, fabrication and testing of the optical system "thick" EA LC SLM - TV control contour.

Tentative cost - 25,000 $

3. Demonstration experiment on NOF-correction with dynamic holographic converter.

Tentative cost - 30,000 $

4. Theoretical and numerical study of system performance and elaboration of technical requirements to the corrector unit and schematics to be used in real imaging telescope.

Tentative cost - 10,000 $

It is supposed that the work can be done in 12 months. The deliveries - quarterly and final reports.